Chem Soc Rev

Carbon Nanomaterials: Multi-Functional Agents for Biomedical Fluorescence and Raman Imaging

Journal:	*Chemical Society Reviews*
Manuscript ID:	CS-REV-09-2014-000306.R1
Article Type:	Review Article
Date Submitted by the Author:	15-Sep-2014
Complete List of Authors:	Bartelmess, Juergen; Istituto Italiano di Tecnologia, Nano Carbon Materials Quinn, Susan; University of Dublin, Chemistry Department Giordani, Silvia; Istituto Italiano di Tecnologia, Nano Carbon Materials

Cite this: DOI: 10.1039/c0xx00000x

www.rsc.org/xxxxxx

ARTICLE TYPE

Carbon Nanomaterials: Multi-Functional Agents for Biomedical Fluorescence and Raman Imaging

J. Bartelmess,[a] S. Quinn[b] and S. Giordani[a*]

Received (in XXX, XXX) Xth XXXXXXXXX 20XX, Accepted Xth XXXXXXXXX 20XX

DOI: 10.1039/b000000x

Carbon based nanomaterials have emerged over the last years as important agents for biomedical fluorescence and Raman imaging applications. These spectroscopic techniques utilize either fluorescently labelled carbon nanomaterials or the intrinsic photophysical properties of the carbon nanomaterial. In this review article we present the utilization and performance of several classes of carbon nanomaterials, namely carbon nanotubes, carbon nanohorns, carbon nanoonions, nanodiamonds and different graphene derivatives, that are currently employed for *in vitro* as well as *in vivo* imaging in biology and medicine. A variety of different approaches, imaging agents and techniques are examined and the specific properties of the various carbon based imaging agents are discussed. Some theranostic carbon nanomaterials, which combine diagnostic features (*i.e.* imaging) with cell specific targeting and therapeutic approaches (*i.e.* drug delivery or photothermal therapy) are also included in this overview.

Introduction

Imaging in Biology and Medicine

The use of nanoprobes as imaging agents is a very promising new development for obtaining detailed images of living systems.[1,2] The combination of drug delivery features with imaging techniques allows the researcher to follow the distribution of the drug inside the organism and gives further hints for the optimization of disease treatment.[3,4] Leading examples in biomedicine include the therapy of cancer. For this purpose, the use of nanomaterials led to promising new approaches for diagnosis and therapy.[5] This combination of diagnostic tools such as imaging with therapeutical approaches gives rise to so-called theranostic nanomaterials. On the forefront of theranostic nanomaterials for cancer therapy are carbon nanomaterials (CNMs) due to their large surface area and other beneficial properties. Carbon nanotubes (CNTs), for example, have shown encouraging results in a multitude of studies.[6,7] In this review article, we summarize and discuss the reported research about CNMs employed in biological or medicinal imaging using fluorescence and/or Raman spectroscopy. There, the CNMs function either as delivery vectors for fluorescent probes or act as imaging agents themselves, due to their intrinsic optical properties.

Carbon Nanomaterials

Several new nanoforms of carbon[8,9] - Scheme 1, have recently been explored in the context of biomedical imaging. The first publication on the "Buckminsterfullerene" C_{60}[10] can be seen as the initial report on the fascinating topic of novel nanocarbons and has led to an unprecedented boom in world-wide research. However, C_{60} has not been widely employed for biomedical imaging purposes and therefore will not be presented here. We will focus on other CNMs, which show much more beneficial properties for applications in this particular research area. Especially carbon nanotubes (CNTs), carbon nanohorns (CNHs), nanodiamonds (NDs), carbon nanoonions (CNOs) as well as graphene and its derivatives were widely employed.

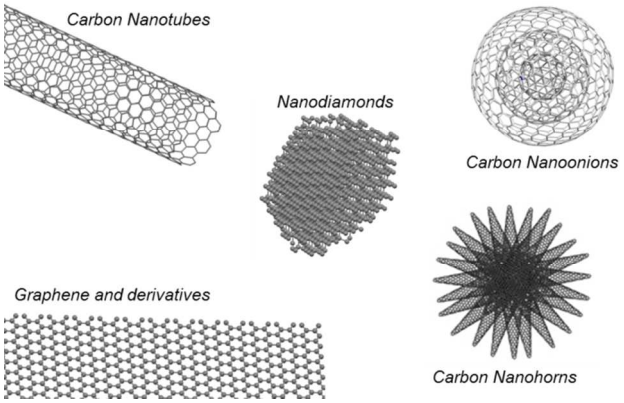

Scheme 1 Structure of CNMs utilized for imaging applications.[11]

Single-wall carbon nanotubes (SWCNTs) are graphene sheets rolled-up to a tubular structure,[12,13,14,15] while multi-wall carbon nanotubes (MWCNTs) are made from several interleaved CNTs. The fabrication of CNTs requires the presence of transition metal catalysts such as Fe or Co and Mo,[16,17] which subsequently needs to be removed from the as-produced raw CNTs. Complex purification procedures are usually necessary to obtain pure CNTs applicable for biological applications.[18,19] Carbon nanohorns (CNHs), which are closely related to CNTs, appear as conical, single-walled carbon nanostructures and are typically

observed in Dahlia-flower like aggregates.[20] CNHs can be produced in high yields by the catalyst-free CO_2-laser ablation of graphite.[21] Nanodiamonds (NDs) are the nano-sized derivative of the well-known diamond, which are usually recovered from detonation soot.[22] The large scale production of fluorescent NDs is possible, intrinsic fluorescence is typically achieved through the introduction of nitrogen vacancies. Different additional techniques for the fabrication of fluorescent NDs, such as the irradiation of diamond nanocrystallites with helium ions[23] or high energy ball milling of diamond microcrystals[24] have been reported. Furthermore, NDs can be used for the preparation of CNOs. CNOs[25] consist of several individual spherical graphitic layers of carbon, usually with a fullerene C_{60}, or one of its larger analogues, in the centre. Several different approaches for the preparation of CNOs were reported.[26] A commonly used method for the production of small CNOs is the thermal annealing of commercially available NDs.[27,28] This method can be used to produce high quality CNOs with diameters of approx. 5 nm in gram scale quantities. Interestingly, the one carbon allotrope from which many of the other CNMs structurally depend on - graphene, a single, two-dimensional sheet of carbon - was reported last.[29] Nevertheless, this nanomaterial has attracted a significant amount of interest in the last years.[30] Graphene is usually prepared by the exfoliation of graphite. Possible methods are the peeling of single graphene layers from bulk graphite in addition to other mechanical ways or physico-chemical exfoliation procedures.[31,32,33] Recently, the large scale production of graphene using surfactants was reported.[34] Chemical Vapour Deposition (CVD) is another possible technique for the preparation of graphene.[35] Based on bulk graphene are several modified derivatives such as graphene oxide (GO) and reduced graphene oxide (RGO).[36,37,38] Also structurally derived from graphene are carbon dots (CDs) or graphene quantum dots (GQDs), which are small, quasi one-dimensional graphene particles and widely used for imaging. They can be prepared by a variety of methods.[39,40] The carving of graphene was reported[41] as well as bottom up methods via direct wet chemical routes.[42,43,44] However, most GQDs / CDs utilized for imaging are synthesized by using hydrothermal methods what will be highlighted in the corresponding section of this review.

The immense research efforts on the various carbon nanostructures led to the development of a large number of synthetic strategies for functionalization. The chemical modification of CNTs,[45,46] graphene,[36,37,38] NDs[47] as well as CNOs[48] was subject of several recent review articles and allows the introduction of a wide variety of different functionalities. Through the optimisation of chemical modifications with small molecules and biomolecules[49] and the coupling with other nanomaterials (*i.e.* luminescent and magnetic), carbon nanomaterials have emerged as a platform for the preparation of sophisticated multi-functional smart materials capable of imaging, recognition and targeting, and drug delivery.

Toxicity of Carbon Nanomaterials

In general, for all biological and medicinal applications, but also for environmental safety, profound knowledge of the toxicity of nanostructures is of great importance.[50] In biomedicine for example, where CNMs are employed as imaging agents or as multi-functional drug delivery vectors in living organisms, a low toxicity is obviously highly desirable. In the case of CNTs, guidelines for their safe use in medicine were suggested.[51] In general, the toxicity of CNTs was subject of a multitude of reports,[52] especially their high aspect ratio has raised particular concern regarding potential asbestos like behaviour.[53] The impact of CNTs on environmental health and workplace safety was widely studied,[54,55] as well as their biocompatibility[56,57,58] including the effects of CNTs on living mammalian cells.[59] To summarize, CNTs have shown negative effects on living organisms. One main reason for this observation seems to be the presence of toxic residual catalyst particles, which makes the diligent purification of CNTs prior to any biological application a necessity. One method to reduce, or even eliminate toxic effects of CNTs is a high grade of surface functionalization, which can be accomplished, for example, by wrapping with polymers or by covalent surface functionalization.[56,58,59] Asbestos-like pathogenicity of long CNTs could also be alleviated by chemical functionalization.[60]

Iijima and collaborators published an extensive study on the i*n vitro* as well as *in vivo* toxicity of CNHs in 2008.[61] It was found that CNHs were non-irritant and also non carcinogenic. Overall, as-grown CNHs revealed a low acute toxicity, which renders them as promising material for biological applications.

The toxicity of graphene and related compounds was subject of several studies, but the data is still very limited.[62,63] Systematical *in vitro* and *in vivo* studies are needed to fully elucidate the toxicological potential of these CNMs. In particular, the generation of reactive oxygen species seems to the reason for some of the observed toxicological effects. Other studies, however, suggest a good biocompatibility of graphene based imaging agents, which will be discussed in the corresponding section of this review, when the structures are presented together with the imaging results. As long as the data is limited, graphene based nanomaterials should be handled with special care and the monitoring of potential toxicological effects should be included in future studies.

NDs have not shown notable cytotoxicity and thus attracted large attention in current research.[64,65,66] The excellent biocompatibility of NDs makes them highly attractive for *in vitro* and *in vivo* applications in biology and medicine.

One early report on the effects of large CNOs (diameter of approx. 30 nm) on the immune system indicated that the cell response was highly dependent on the size of the carbon nanomaterial.[67] Small diameter CNOs did not reveal any cytotoxic effects.[68,69] We recently reported that small surface functionalized CNOs (diameter of approximately 5 nm), compared with similarly functionalized CNTs, reveal a low cytotoxicity and inflammatory potential, thus rendering them a good candidate for biological applications.[69] Nevertheless, the limited data on CNO toxicity makes it necessary to routinely study possible cytotoxic effects in future research projects, especially when altering the CNOs' substitution patterns and target organisms.

In general, and even if toxicological studies suggest their safety, all CNMs should be handled with great care and especially the exposure to and the inhalation of dusts should be prevented.

Techniques and Methodologies for Imaging

The following section will give the reader an overview over different aspects of biomedical imaging using optical techniques such as fluorescence and Raman spectroscopy. First, some general aspects of fluorescence imaging in biological systems are discussed. Following this, the intrinsic fluorescence properties of the various CNMs are briefly summarized and approaches for the functionalization of CNMs with fluorescent labels are presented. In addition, the characteristic, strong Raman scattering properties of CNMs are introduced, which consequently renders Raman spectroscopy as a powerful technique for biological imaging.

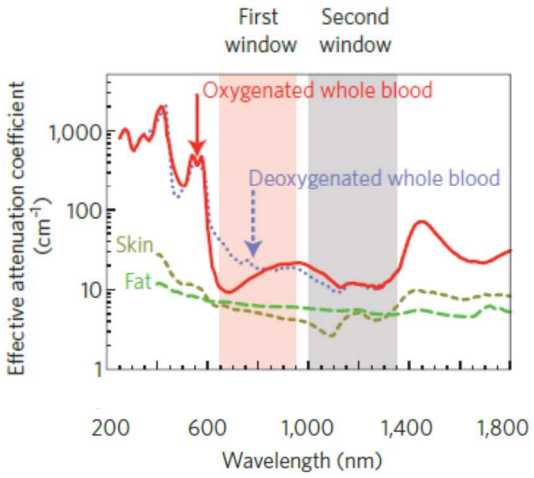

Fig. 1 Optical NIR windows in biological tissues. Reprinted by permission from Macmillan Publishers Ltd: Ref. 71. Copyright (2009).

Biological Window

Many organic fluorophores absorb and emit light in the visible spectral range which can have some drawbacks. In complex biological systems like cells, or especially in living organisms, the absorption and autofluorescence of the tissue and body fluids is a major problem for optical imaging. The absorption reduces the transmission of the excitation light and also the emitted fluorescence signal is significantly weakened, or even completely quenched. To overcome this issue, researchers have found that in the NIR region between 650 – 950 nm, the so-called NIRI, haemoglobin and water, as the two main absorbers, have low molar extinction coefficients.[70] NIR light can penetrate the tissue and the use of NIR emitting dyes with emission maxima in the NIRI as fluorescent labels allows for deep tissue imaging. Another optical window, the NIRII, has been identified later in the spectral range between 1,000 and 1,350 nm – See Figure 1.[71,72] However, until the discovery of NIR fluorescent CNTs, biological imaging in the NIRII was limited due to the lack of available fluorophores. In the corresponding section of this review article, various approaches for the application of NIR fluorescent CNTs will be presented and discussed. Also Raman imaging is typically performed in the NIRI or NIRII.

Intrinsic Fluorescence of Carbon Nanomaterials

Several spectroscopic techniques can be utilized for biological *in vitro* and *in vivo* imaging. One of the most common techniques is fluorescence imaging. CNMs can be used for their intrinsic fluorescence properties or can be tagged with fluorescent molecules.

Several carbon nanomaterials are known to emit fluorescence light upon photo-excitation. The leading example are semiconducting SWCNTs, which show a structure dependent fluorescence in the biological important NIRII window, which has been widely studied.[19,73,74,75,76,77,78,79] The purity and chirality of the utilized SWCNTs play thereby an important role. The band gap fluorescence of semiconducting SWCNTs originates from light absorption at a photon energy of E_{22}, creating an electron-hole pair. This initial excitation is followed by a non-radiative relaxation of the electron to the conduction band and then the fluorescence event with a photon energy of E_{11} – See Figure 2.[80] The fluorescence quantum yields of SWNTs are low, typically <0.01 for macroscopic samples of SWCNT,[81,82] and show a strong dependency on environmental factors. For very well dispersed, individual SWCNTs higher fluorescence quantum yields of up to 0.07 have been reported.[83] Recent advance in chemical doping of SWCNTs through oxygen[84] or sp^3 incorporation[85] has led to largely increased fluorescence quantum yields. Also in the visible region, fluorescence of well-dispersed CNTs was reported, which shows a large dependence on the type of the CNT functionalization.[86,87,88]

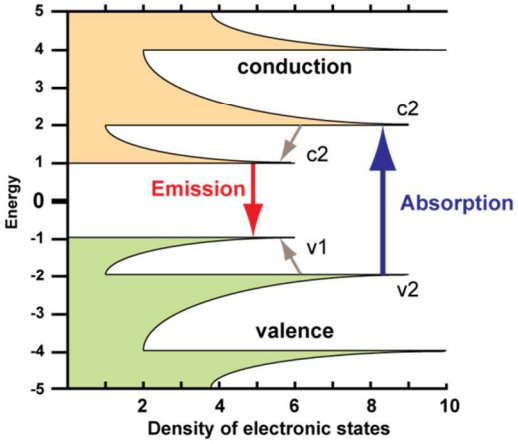

Fig. 2 Schematic representation of the density of states for a single carbon nanotube illustrating the transitions leading to SWCNT fluorescence. Reproduced with modifications from ref. 80.

Another example for fluorescent CNMs are GQDs/CDs which were used by a large number of research groups for biological imaging applications, as shown later in this review. The mechanisms of the GQD fluorescence is currently under investigation and still, the physical origin of the fluorescence seems not to be fully understood and is subject to scientific controversy.[89,90,91,92] However, it is certain that structurally perfect, defect free bulk graphene does not show luminescence upon photo-excitation. One common strategy toward the creation of fluorescent graphene derivatives is the manipulation of the π-network by the introduction of sp^3-hybridized carbons, *e.g.* the formation of defect sites.[93] An interesting feature of GQDs is their excitation wavelength dependent emission. In line with

modulation of the excitation wavelength, the emission wavelength undergoes a shift.[94] In a recent study, the group of Wu leads this dependency in GO nanoparticles back to a "giant red-edge effect", induced by slow solvent relaxation processes between polar solvent molecules and photo-excited GO.[95]

The intrinsic fluorescence emission of NDs, which can be led back to the presence of nitrogen-vacancy centres in the structure of the NDs,[96] is also widely utilized for fluorescence imaging. Recent advances in the control over the formation of nitrogen-vacancy centres led to ultra-bright NDs with improved emission properties.[97]

Finally, CNOs are also fluorescent, however, the fluorescence of CNOs was just discussed in a few studies. A first study by Guldi, Bozio and Prato in 2003 reported fluorescent functionalized CNOs with an emission wavelength of 480 nm upon excitation at 380 nm and a fluorescence quantum yield of 0.08.[98] Interestingly, a shift of the excitation wavelength led to a shift of the emission wavelength as well. The same groups reported comparable fluorescence features a few years later.[99] A last report about fluorescent CNOs by the group of Sarkar in 2011, describes the fluorescence of CNOs prepared by the pyrolysis of wood wool and subsequent oxidation with nitric acid.[100] The mechanism of CNO fluorescence, however, is not known. The excitation wavelength dependency might point toward a mechanism similar to the one seen for GQDs. Surprisingly, not many studies about CNOs even report CNO centred fluorescence, so possibly the CNO production process and thus the specific properties of CNOs such as size as well as defect sites influence the emissive behaviour of CNOs. Also the CNO functionalization might play an important role. To fully understand the emissive properties of CNOs, detailed future studies seem to be highly desirable.

Fluorophore Functionalized Carbon Nanomaterials – Covalent vs. non-Covalent Functionalization

The attachment of fluorophores to create fluorescent nanostructures, suitable for biological imaging is well established. Both the covalent and non-covalent functionalization approaches are widely used. Covalent functionalization is, in general, accomplished by the chemical functionalization of the carbon backbone of the CNM.[45,46] Various methods for the functionalization of CNMs have been described in detail previously. Important for the development of novel functionalized CNMs is the observation, that quite often reactions, described for one CNM, can be adopted for the functionalization of other CNMs. This can be depicted readily for example on a well known reaction, that is the CNM functionalization *via* diazonium chemistry, *i.e.* the radical addition of phenyl groups to the graphitic sidewalls of the carbon nanostructure – See Scheme 2. This reaction was first described for the functionalization of highly ordered pyrolytic graphite (HOPG)[101], shortly after for CNTs by Tour *et al.*[102,103] and in the following years the reaction was employed for the functionalization of CNOs,[104] NDs,[105,106] and graphene.[107,108] Covalent functionalization goes in line with structural changes of the carbon backbone and eventually leads to the quenching of the intrinsic fluorescence, which has been demonstrated for example for SWCNTs and diazonium compounds by Cognet *et al.*.[109]

The non-covalent approach for the functionalization of CNMs is typically accomplished by means of π-π-stacking, hydrophobic or van-der-Waals interactions and it is well described, for example, in the case of CNTs.[110,111] Agents for the non-covalent surface functionalization can act either as surfactants, forming micelles or being wrapped around the CNM or they can function as anchoring groups, promoting the surface immobilization of other compounds such as dyes, targeting moieties or solubility enhancing building blocks. Typical compounds utilized for the non-covalent surface functionalization of CNMs are small molecules such as pyrene[112,113,114] or sodium dodecylsulfonate (SDS)[73] but also oligomeric structures,[115,116] polymers,[117,118] nucleic acids,[119,120,121,122,123] and proteins.[124] Moreover, drugs such as doxorubicin (DOX) or sensitizers for photodynamic therapy such as Photochlor®, which show fluorescence applicable for imaging, can be immobilized on the surface of CNMs. Some examples will be discussed later in this review article. In contrast to covalent CNM functionalization, the electronic structure of the CNMs is not altered in the non-covalent approach.

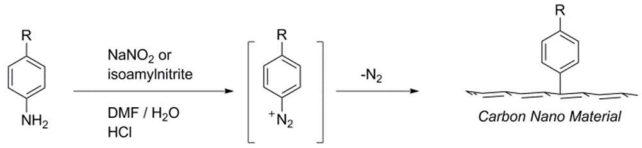

Scheme 2 Covalent functionalization of CNMs with *in situ* generated diazonium salts.

Fluorescence Quenching in Labelled Carbon Nanomaterials

The emission of fluorescence labelled CNMs is largely dependent on the chemical and photophysical nature of the implemented fluorophores. In addition, the linkage between the fluorophores and CNMs can play an important role, since it influences largely the interaction between the building blocks. In most cases, the emission intensity of a fluorophore bound to a CNM is lower than the one of the free dye in solution. In the corresponding section of this review article, several examples will be presented where this effect is observed. Typically, the remaining fluorescence signal is intense enough for cellular imaging. The reduced fluorescence intensity can be led back to a high intrinsic absorption of the CNMs, especially when taking into account that most CNMs show plasmonic absorption over the whole spectral range. On the other hand, the quenching of the fluorophores photo-excited states by the CNM is observed. This can be due to different kinds of electronic interactions, involving energy or electron transfer events from the photo-excited chromophore to the CNM or *vice versa*. Amongst many examples in literature, typical CNM based systems showing photo-induced electron transfer consist of CNTs in combination with phthalocyanines,[114,115,116,125] porphyrins,[112,113,126,127,128] and also boron azadipyrromethenes.[129] Many of these CNT-dye-conjugates were successfully probed in antenna systems for solar cell application. For imaging, this fluorescence quenching is obviously a large drawback, which was overcome by developing synthetic strategies to electronically separate the fluorophore from the CNM. This can be accomplished, for example, by the introduction of molecular spacers, biomolecules or coatings between the fluorophore and the CNM. Various examples illustrating this concept will be discussed in the corresponding sections of this review article, which highlight fluorescently labelled CNMs.

Raman Spectroscopy of Carbon Nanomaterials

Raman spectroscopy is a versatile tool for the characterization of sp^2 carbon nanomaterials such as CNTs and graphene[130,131] as well as CNOs.[132] Also in several fields of nanomedicine, Raman spectroscopy is applied for diagnostics and imaging.[133,134] In the biomedical field, however, only CNTs are widely used, as we will illustrate in the corresponding section of this review article. Some additional reports employ NDs as Raman active agents for imaging. The various Raman modes of CNTs - See Figure 3 - originate in their unique structure of a single graphene sheet, rolled up to a tube.[135] The most distinctive Raman modes observed are the radial breathing modes (RBMs) at low wavenumbers[136] and the G and G' band at higher wavenumbers.[130,131,135] In addition, disruptions of the CNTs graphitic sp^2 backbone result in the formation of the so-called D-band. The intensity of the D-band represents the amount of the CNTs defect sites (*i.e.* sp^3 hybridization) and is commonly utilized as measure for the grade of covalent CNT functionalization. For biomedical applications, the intensity of the G-band at around 1593 cm^{-1} is monitored as direct measure for the CNT distribution inside the biological structure,[133,134] but also the RBMs (between 75 and 300 cm^{-1}) are used for imaging applications.[75] A useful characteristic of CNTs is that different ratios of ^{12}C to ^{13}C in the CNTs lead to shifts of the Raman bands, allowing for two- or multi-colour imaging.[137,138,139] Since sample irradiation in Raman spectroscopy can be accomplished with IR laser sources, *in vivo* deep tissue imaging is possible and has encouraged ambitious research efforts in the field of biomedical imaging, as will be illustrated later. These two aspects render SWCNT Raman imaging an interesting complementary technique to fluorescence imaging, even if the Raman effects of CNMs are quite weak and the cross section is very small for imaging purposes. Recent developments in this field include the incorporation of dyes in the internal cavity of SWCNTs, which gives rise to improved imaging properties and giant resonant Raman scattering effects.[140]

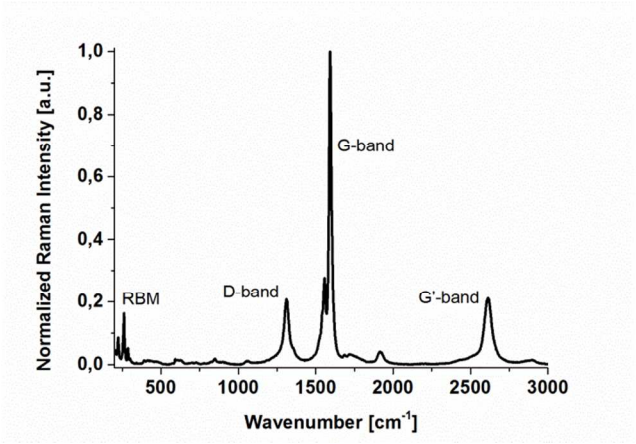

Fig. 3 Representative Raman spectrum of purified, covalently functionalized SWCNTs prepared by the high pressure CO conversion (HiPCO) process.

Other Imaging Techniques

In addition to imaging techniques based on optical and vibrational spectroscopies, which are discussed in this review, some other imaging techniques are common in biomedicine. Leading examples include magnetic resonance imaging (MRI), photoacoustic tomography (PAT) and techniques using radionuclides such as positron emission tomography (PET). In these cases, several examples employing CNMs as imaging agents are reported.[141,142,143,144,145]

Imaging with Fluorescently Labelled Carbon Nanomaterials

Fluorescently Labelled Carbon Nanotubes

Carbon nanotubes are widely employed in biomedical applications such as drug delivery due to their advantageous properties like a high surface area.[6,7,146] Along with drug delivery

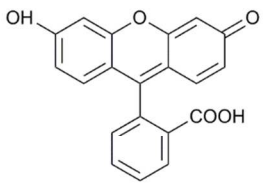

Fluorescein
(core structure)

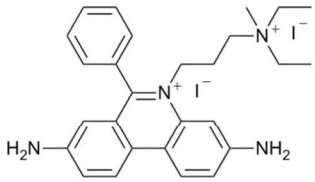

Propidium Iodide

features comes in many cases the incorporation of fluorescent molecules for imaging. Especially fluorescein derivatives are widely used as fluorescent labels in combination with CNTs. An early examples of fluorescein labelling originates from 2004 when the groups of Prato and Bianco used fluorescein tagged SWCNTs to follow the internalization of the CNTs by human 3T6 and murine 3T3 fibroblasts.[147] In another study from the same year, Kam *et al.* reported the successful uptake of different SWCNT derivatives (including fluorescein labelled SWCNTs for imaging) into human promyelocytic leukaemia (HL60) cells, in addition to other cell lines.[148] Just one year later, Bianco and collaborators utilized fluorescein tagged SWCNTs for the targeted delivery of Amphotericin B, an antifungal drug.[149] The investigated mammalian cells readily internalized the SWCNTs and no toxic effects were observed. The antifungal activity, however, was preserved and the fluorescent Amphotericin B / fluorescein / SWCNT conjugates were still effective against several strains of clinically relevant fungi. In the following years, the cellular uptake mechanisms of functionalized CNTs were studied in detail.[150] It was shown that covalently functionalized CNTs, bearing different fluorescein based labels for imaging in addition to other functional groups, were uptaken by a variety of different cell lines. In this regard, the exact nature of the CNT functionalization did not seem to be of great importance. The authors lead this facile cellular uptake by both mammalian as well as prokaryotic cells back to the cylindrical shape and high aspect ratio of the CNT nanomaterial, which enables penetration of the cell membranes. Several research groups investigated the significance of CNTs as vectors for drug delivery. Combining drug delivery with fluorescence labelling the presented CNT derivatives are excellent examples for theranostic nanomaterials. Two consecutive studies were published by the groups of Dai and Lippard, where a Pt(IV) prodrug was delivered into cells by

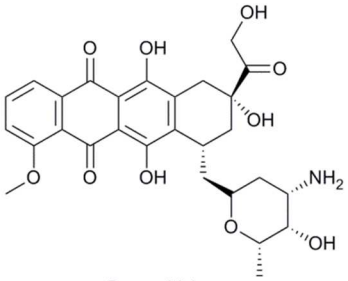

Doxorubicin
(DOX)

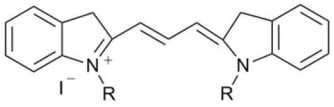

Cyanine Dye 3
-basic structure-
(Cy3)

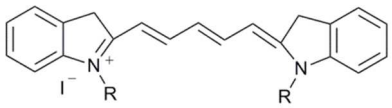

Cyanine Dye 5
-basic structure-
(Cy5)

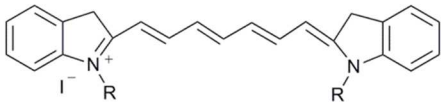

Cyanine Dye 7
-basic structure-
(Cy7)

utilizing SWCNTs.[151,152] *In vitro* fluorescence imaging of NTera-2 testicular carcinoma cells was accomplished by the incorporation of a fluorescein based fluorophore in the CNT-Pt(IV) system.[151] In a follow-up study, the authors added a folic acid moiety for targeting folate receptor-enriched tumour cells. Again, *in vitro* imaging was achieved by monitoring the luminescence of fluorescein fluorophores on the SCWNTs.[152] Other pharmaceutically active molecules, which were transported into cells by utilizing SWCNTs were oligonucleotides,[121] methotrexate (MTX),[153] the second generation taxoid SB-T-1214,[154] and DOX.[155] In all these examples, fluorescein labels were used to track the drug delivery systems inside the cells. In the latter study, Heister and collaborators reported a multifunctional targeted drug delivery system.[155] Targeting was accomplished by antibody tagged bovine serum albumin (BSA), which was also labelled with fluorescein for cellular imaging – See Figure 4. In addition to the green fluorescein fluorescence (measured between 500 and 530 nm), also the red intrinsic fluorescence of DOX (measured between 650 and 710 nm) can be observed in the cells and allows for multicolour imaging. Recently, our group reported the covalent functionalization of benzoic acid groups on SWCNTs (prepared by the so-called Tour reaction)[104] with fluorescein amine by an amidation reaction.[69] These fluorescent SWCNTs were used for *in vitro* imaging of different cell lines. The cytotoxicity was compared with similarly functionalized CNOs, which are discussed later in this review.

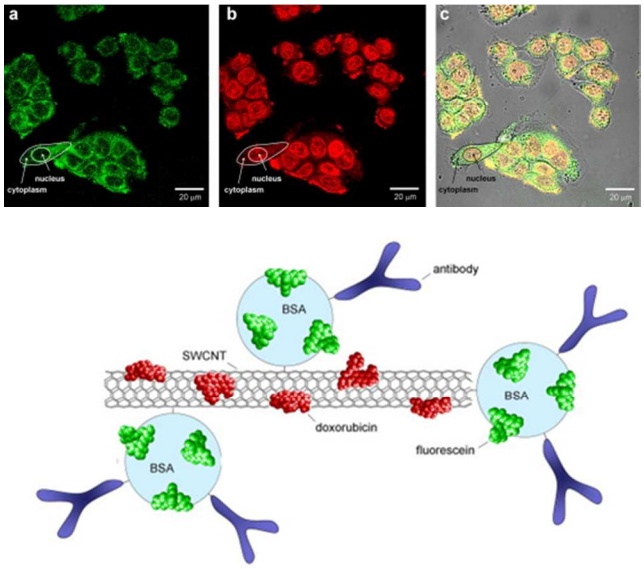

Fig. 4 Schematic illustration of the doxorubicin–fluorescein–BSA–antibody-SWCNT complexes (top). Colour code: red = doxorubicin, green = fluorescein, light blue = BSA, dark blue = antibodies. Confocal image of WiDr cells incubated with doxorubicin–fluorescein–BSA–SWCNT complexes (a = emission measured at 500–530 nm (fluorescein), b = emission measured at 650–710 nm (doxorubicin), and c = transmitted light image showing all channels) (bottom). Reprinted from Ref. 155, copyright (2009), with permission from Elsevier.

The group of Dai reported one example for non-covalently functionalized, fluorescein labelled SWCNTs.[118] Fluorescein functionalized polyethyleneglycol (PEG) was physiosorbed onto the surface of SWCNTs, affording stable aqueous suspensions. Incubation of BT474 breast cancer cells with this fluorescent nanomaterial led to an internalization of the SWCNTs, which was proven by confocal microscopy, among other methods. Also DNA, labelled with fluorescein isothiocyanate was used to functionalize SWCNTs non-covalently and to monitor the cellular uptake of the carbon nanomaterial by confocal microscopy.[156]

Complementary to the example mentioned previously, where fluorescein was used in combination with DOX for intracellular imaging,[155] other studies were reported where just the intrinsic fluorescence of DOX was used as fluorescence tracker. In one example, the group of Dai loaded DOX on different water-soluble CNTs and studied the cellular uptake of this nanomaterial by UM87G and MCF-7 cells.[157] The fluorescence of DOX was sufficient for confocal fluorescence imaging of the investigated cells. In 2009, Lu and co-workers extended the concept of non-covalent CNT functionalization with DOX by adding folic acid as targeting moiety.[158] SWCNTs were functionalized with sodium alginate and chitosan polymers, then folic acid was tethered to the CNTs and DOX was loaded. The fluorescence of DOX allowed for intracellular imaging and tracking of the drug delivery system. In addition to fluorescein, other commercially available fluorophores were used for the labelling of CNTs and *in vitro* cellular imaging. The cellular uptake of nucleic acid - RNA polymer poly(rU) functionalized CNTs into MCF-7 breast cancer cells was followed by labelling the SWCNT / poly(rU) hybrids with propidium iodide, which is known to interact with the base

pairs of nucleic acids.[120] Another fluorophore applied for the labelling of DNA, which then was non-covalently attached to SWCNTs is Cyanine3 (Cy3). The investigated cells from different cell lines internalized the functionalized SWCNTs and the uptake was confirmed by confocal microscopy tracking the intense fluorescence signal of Cy3.[156,159,160] In 2011, the group of Ray showed that gold nanopopcorn attached to SWCNTs is suitable for targeted diagnosis and photothermal therapy.[161] For imaging purposes, Cy3 modified S6 aptamers attached to the functionalized SWCNTs, were employed. When SWCNTs were used as intracellular transporters for proteins such as BSA and streptavidin (SA), fluorescence labelling was accomplished by using the commercial dye Alexa Fluor 488.[124,156]

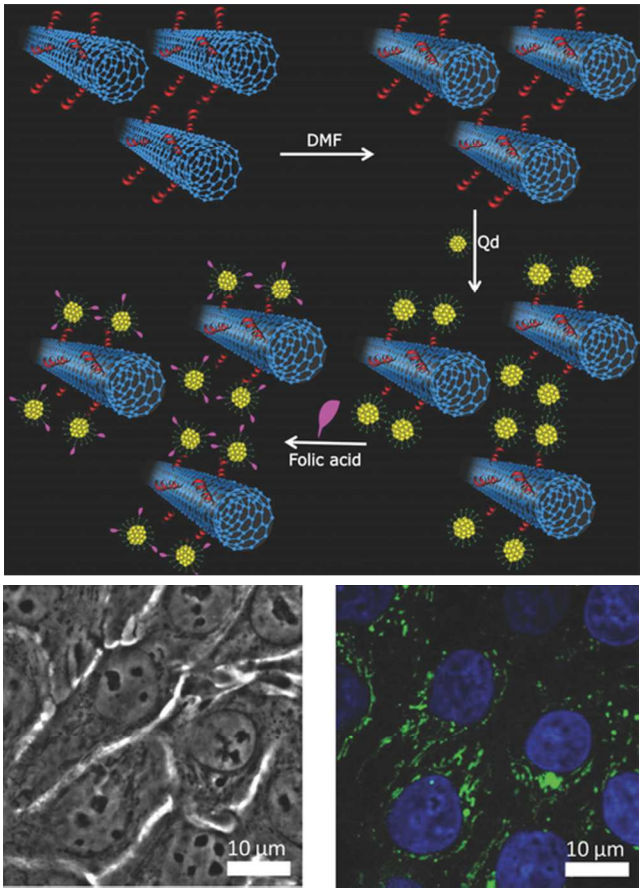

Fig. 5 Schematic representation of the folic acid tagged, SWCNT-QD hybrid nanosystem (top). Cellular uptake of folic acid functionalized SWCNT-QD particles by MCF-7 cells (bottom). Reprinted from Ref. 171 with permission from John Wiley and Sons, copyright (2014).

Fluorescent quantum dots (QDs) and related nanocrystalline materials have been widely studied for biological applications. Their tuneable, bright fluorescence, together with their robustness renders them ideal for bioimaging.[162,163,164] Also in combination with CNTs as delivery systems, QD were successfully employed as fluorescent tags. An early example originates from 2006, when Bottini *et al.* reported the decoration of SWCNTs with streptavidin and conjugated to this protein CdSe/ZnS core shell QDs.[165] The fluorescence signal of the QDs was observed by confocal microscopy inside the cells (Jurkat T leukemia cells), confirming cellular uptake of the nanomaterial and subsequently illustrating its transport into lysosomes. In another study CdSe/ZnS QDs were immobilized on the surface of oxidized MWCNTs by an amidation reaction.[166] The fluorescent nanomaterial was then injected hypodermically in living nude mice. The QDs were detected by fluorescence microscopy *in vivo*. In addition to CdSe/ZnS QDs, NIR emitting InGaP/ZnS QDs were used to overcome autofluorescence and light absorption of the tissue and allow for deep tissue imaging. A different approach for the immobilization of CdSe/ZnS QDs was presented by the group of Tang, which firstly functionalized oxidized MWCNTs with polyamidoamine (PAMAM) dendrimers and then subsequently attached the QDs.[167] This fluorescent nanomaterial was used for the imaging of HeLa cells without showing large effects on the cell viability. Very recently, Wang, Cui and co-workers reported a fluorescent, surface enhanced Raman scattering encoded, and magnetic SWCNT based multi-functional nanomaterial.[168] The authors incorporated several kinds of nanoparticles, including Au nanoparticles, superparamagnetic iron oxide nanoparticles (SPION) and water soluble mercapto propionic acid capped CdSe/ZnS QDs. The cellular uptake of this nanomaterial by MCF-7 and SKBR3 cells was shown and verified by confocal microscopy.

Also in the field of theranostic nanomaterials, CNTs labelled with fluorescent QDs were developed. A SWCNT based delivery system for the anticancer drug cisplatin was reported by Bhirde *et al.*.[169] The authors prepared multi-functional SWCNTs bearing several building blocks including epidermal growth factor for targeting, a cisplatin derivative for therapy, and commercially available amino (PEG) QD nanocrystals (Qdot605) for imaging. The theranostic nanomaterial was found to selectively target epidermal growth factor overexpressing cancer cells and showed promising anti-cancer efficiency *in vitro* as well as *in vivo*. Another multi-functional CNT based drug delivery system with CdTe QDs for bioimaging was presented by the groups of Chen and Wang in 2012.[170] Magnetic Fe_3O_4 nanoparticles were deposited inside the CNTs, while their surface was decorated with targeting units, QDs for imaging and the anti-cancer drug DOX. The fluorophores, SiO_2-coated CdTe nanocrystals, were attached to the SWCNTs and showed a bright fluorescence signal suitable for cellular imaging. The SiO_2 shell largely prohibited fluorescence quenching by the carbon nanostructure. In addition to the QD luminescence, also the emission of the SWCNT adsorbed DOX was suitable for imaging. A very recent example for QDs in multi-functional SWCNT based systems are CdSe/ZnSe QDs, stabilized by cysteine, which were attached to the surface of SWCNTs – See Figure 5.[171] Folic acid was bound to the QDs for targeting folate receptor overexpressing cells. Different cell lines (mice fibroblasts L929, MCF-7 breast cancer cells and Panc1 pancreas cancer cells) were used for cellular uptake experiments and showed good cell viability of over 80% after 24 h. To illustrate the photothermic potential of the nanomaterial, the cells were irradiated with laser light of a wavelength of 800 nm. Especially the folic acid functionalized QD/SWCNTs revealed excellent results.

Fluorescently Labelled Nanodiamonds

As mentioned previously, modified NDs are known to emit intrinsic fluorescence. Imaging with this fluorescent NDs will be discussed later in this review article. Nonetheless, some reports

refer to NDs functionalized with fluorescein and other dyes for cellular imaging. In a report from 2008 by the group of Hwang, magnetic, iron nanoparticle functionalized NDs were used for the imaging of HeLa cells.[172] Fluorescein was crafted onto the surface of the NDs by firstly attaching poly(acrylic acids) and then subsequently fluorescein *o*-methacrylate. The functionalized NDs were readily uptaken by the cells and the bright green luminescence of the fluorescein dye was observed inside the cells. Vial et al. prepared NDs with an excellent stability in aqueous solution by coating the surface of NDs by silanization or by polyelectrolyte grafting.[173] Then a fluorescein labelled tripeptide was attached. The cellular uptake of the functionalized NDs by Chinese hamster ovary (CHO) cells was investigated by confocal microscopy. It turned out that the NDs were nontoxic and efficiently uptaken by the CHO cells, where they were embedded in the actin cytoskeleton. A ND based drug delivery system was presented three years later by Zhang *et al.*.[174] Toward this, NDs were functionalized with an anti-EGRF antibody as targeting moiety and a fluorescein labelled drug-oligonucleotide conjugate. The cellular uptake of the nanoparticles was investigated by using MCF-7 cells and MDA-MB-231 cells, which overexpress the receptor for the anti-EGRF. By comparing the fluorescein centred fluorescence intensity inside the cells, the authors could verify the presence of NDs in both cell lines, but in much higher concentration in the MDA-MB-231 cells, corroborating successful targeting by means of cellular imaging. Ho and collaborators reported another ND based theranostic drug delivery system recently.[175] DOX loaded NDs were investigated *in vitro* as well as *in vivo* for their efficiency in cancer therapy. The advantages are thereby a reduced *in vivo* toxicity, compared to standard DOX treatment, and a reduced drug efflux from cells treated with ND-DOX, what resulted in an increased killing-efficiency of the anti-cancer drug. Cellular and *in vivo* imaging of wild-type FVB/N mice was accomplished in various ways by either observing the intrinsic fluorescence of DOX or by functionalizing the NDs with the commercial NIR dye XenaFluor 750™. Recently, Salaam and collaborators presented another ND-DOX drug delivery system with a peptide as targeting moiety for $\alpha_2\beta_1$ integrins overexpressing prostate cancer cells.[176] A significant increase in cell death was observed when combining the ND-vector with DOX, compared to DOX alone. Fluorescence imaging was accomplished by using a fluorescein labelled peptide.

Fluorescently Labelled Carbon Nanoonions

Reports discussing fluorescence labelled CNOs, as materials for biological imaging are rare. In 2013, our group presented a first example of CNOs bearing a fluorescent molecule for cellular imaging.[69] Fluorescein amine was covalently attached to benzoic acid functionalities on the surface of the CNOs by an amidation reaction. The fluorescein labelled CNO nanomaterial showed intense fluorescence emission and was suitable for *in vitro* imaging of immortalized bone-marrow mouse macrophages (iBMM) and mouse bone-marrow-derived dendritic cells (BMDCs) – See Figure 6. The CNOs showed weak inflammatory potential and low cytotoxicity *in vitro* and *in vivo*. In a recent study we investigated the use of a different fluorophore. [177]

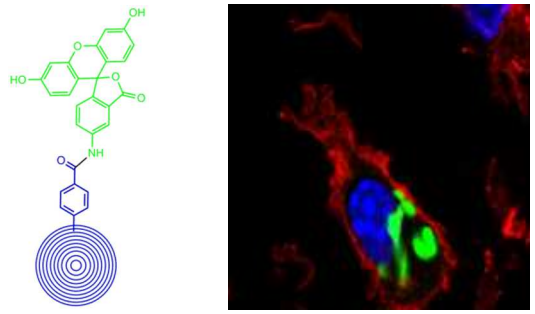

Fig. 6 Fluorescein labelled CNOs utilized for cellular imaging of C57BL/6 BMDCs. Fluorescein labelled CNOs (green), Alexa Fluor 594 (red), Hoechst 33342 nuclear stain (blue). Reprinted from Ref. 69 with permission from John Wiley and Sons, copyright (2013).

A *meso*-phenol boron dipyrromethene (BODIPY) derivative was bound covalently to benzoic acid groups on the CNO surface by an esterification reaction. The CNO nanomaterial showed BODIPY centred luminescence and was applied for the high-resolution imaging of MCF-7 cells with excellent results - See Figure 7 left. Fluorescence imaging of the BODIPY-CNOs, in combination with a lysotracker dye, revealed that the nanomaterial localised in the lysosomes, without showing cytotoxicity.

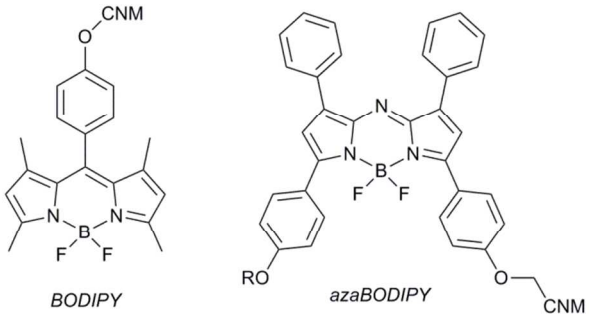

In another approach, we covalently functionalized CNOs with NIR emitting boron azadipyrromethene (aza-BODIPY) derivatives.[178] HeLa Kyoto cells readily internalized the fluorescent CNOs and an intense aza-BODIPY centred fluorescence in the cytosol could be detected by confocal microscopy – See Figure 7 right. CNOs functionalised with an aza-BODIPY derivative bearing a hydroxy- functionality, showed pH dependent fluorescence on-off switching after being internalized by the cells. [179]

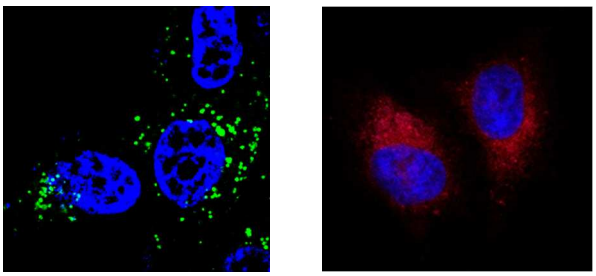

Fig. 7 Confocal microscopy images of BODIPY-CNO (+ Hoechst 33342) labelled MCF-7 cells (left) and azaBODIPY-CNO (+Hoechst 33342) co-labelled HeLa Kyoto cells (right). Reproduced from Ref. 177 and 178 with permission from The Royal Society of Chemistry.

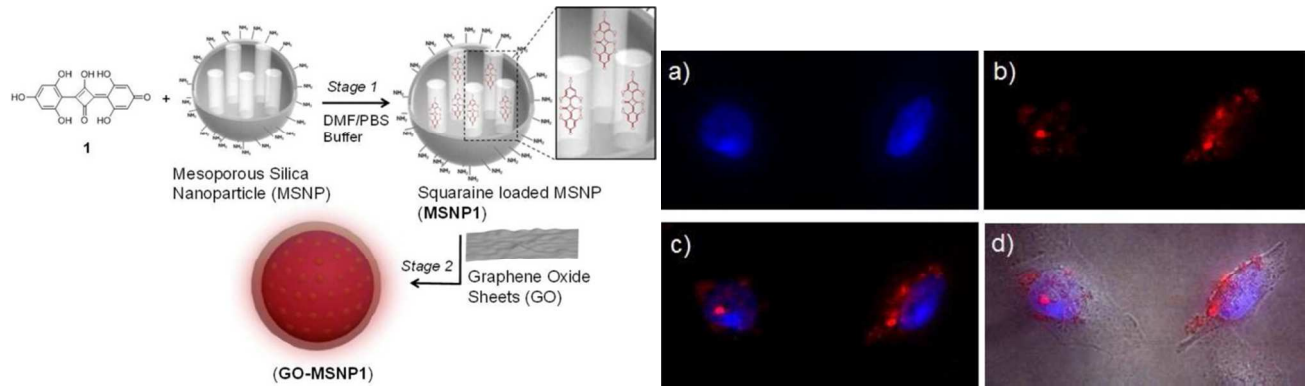

Fig. 8 Schematic representation of the preparation of squarine loaded mesoporous silica nanoparticles, wrapped in GO (left). Epifluorescence microscopy images of HeLa cells labelled with GO wrapped mesoporous silica NPs (right). Blue fluorescence originates from DAPI nuclear stain and red fluorescence from the GO-mesoporous silica NPs. Reprinted with permission from Ref. 183. Copyright (2012) American Chemical Society.

Fluorescently Labelled Graphene Derivatives

Graphene nanomaterials are at the centre of enormous worldwide research efforts. So not surprisingly, sophisticated graphene based systems capable of targeting and drug delivery, in line with cellular imaging, have been reported.

Fluorescein functionalized GO for intracellular imaging was reported by the groups of Fang and Huang in 2011.[180] PEG_{2000} was attached in a first step to carboxylic acids on the GO and subsequently a fluorescein derivative was connected to the PEG spacer. The fluorescent GO nanomaterial was readily internalized by HeLa cells, which was verified by confocal microscopy, and showed no significant cytotoxicity, similar to the unlabelled PEGylated GO.

Chen and Wang published a report where fluorescent GQDs were used in combination with polymer coated RGO.[181] To overcome fluorescence quenching due to excited state interactions of the GQDs with the RGO, the QDs were capped with BSA, which was then grafted onto the RGO. Cellular uptake of this highly fluorescent nanomaterial by HeLa cells was confirmed and no cytotoxicity was observed. Other nanoparticles (NPs) used for the functionalization of GO were Fe_3O_4 NPs, which were precipitated on the GO from solution.[182] The authors report, that the functionalized GO was readily uptaken by T47D cells and the blue GO centred luminescence of the Fe_3O_4 NPs allowed for cellular imaging. Another useful feature of the Fe_3O_4 NPs is their applicability as contrast agent in MRI, which was studied as well in this report. These results render the GO / Fe_3O_4 NPs hybrids as useful dual-mode contrast agents for biological imaging. A third example for NP functionalized GO was reported by the group of Zhao.[183] In this study, mesoporous silica NPs were loaded with a squarine dye as fluorophore and subsequently wrapped in GO sheets – See Figure 8. The nanohybrid material was strongly fluorescent and interestingly, the dye emission was not quenched by typical biological fluorescence quenchers such as cysteine and glutathione. Or in other words, the fluorophore was protected from environmental influences since it was encapsulated in the mesoporous silica NPs / GO. The GO hybrid material was readily internalized by HeLa cells and the red fluorescence of the squarine dye was observed in the cells' cytoplasm. No significant cytotoxicity was reported. Also quantum rods, immobilized on the surface of GO were probed for biological imaging. In a first step, Cd^{2+} cations were adsorbed on the GO, then the ligand 8-hydroxyquinoline was added and the cadmium quantum rods (CdQ_2) formed *in situ* on the GO.[184] The CdQ_2 / GO composite material was highly fluorescent and cellular uptake experiments (in Hep G2 cells) render it suitable for biological applications, especially due to its low cytotoxicity and high photostability. In 2011, the group of Irudayaraj published an interesting approach toward a fluorescent RGO nanomaterial.[185] The authors report a one-step process for the reduction of GO and its surface decoration by using the biomolecule Herceptin. The protein functionalization prohibited the RGO from aggregation, even at high concentrations of NaCl, and led to a water-soluble nanomaterial. The fluorescence of Herceptin could be detected under two-photon excitation, which made the photoluminescent Herceptin-RGO nanomaterial suitable for cellular imaging of SK-BR-3 cells without showing significant cytotoxicity.

PEGylated nanographene sheets (NGS) were used in an *in vivo* study on tumour-bearing 4T1 mice in 2010 by the group of Liu.[186] Fluorescence imaging was accomplished by using the cyanine dye 7 (Cy7) as fluorescent tag. The fluorescence labelling allowed for *in vivo* fluorescence imaging and confirmed a high uptake of the fluorescent PEGylated NGS by the tumour. In addition to this efficient passive tumour targeting, the presented CNM revealed a relatively low retention in reticuloendothelial systems. *In vivo* photothermal tumour therapy was accomplished by irradiation with NIR light. Gollavelli and Ling published another example for *in vivo* imaging with multi-functional fluorescence labelled graphene in 2012.[187] In a first synthetic step, the graphene was magnetized with iron particles by reacting it with ferrocene in the microwave. In a second step, an acrylic acid based polymer was introduced, which promoted water-solubility while in the third step a fluorescein derivative was attached to the graphene as fluorescence tag. The multi-functional nanographene was studied *in vitro* in HeLa cells and *in vivo* in zebrafish as imaging probe and did not induce significant toxicity or other negative effects.

Graphene nanomaterials have also been studied as drug delivery systems. In these cases the drugs for photodynamic therapy

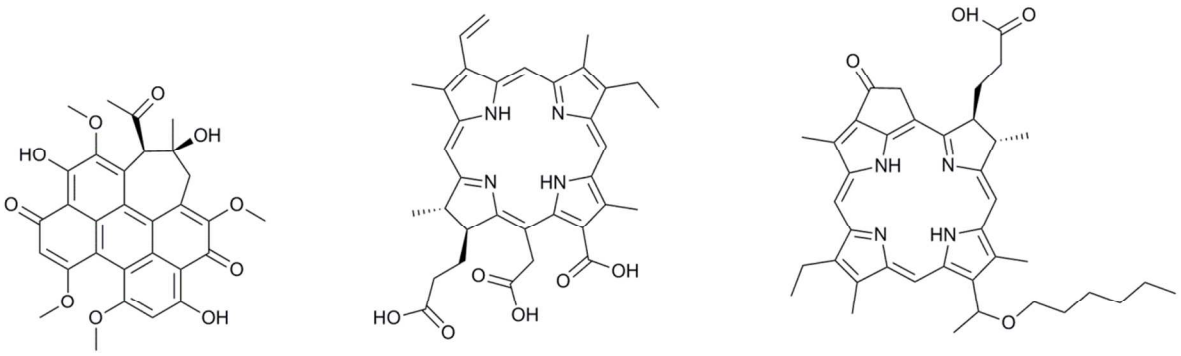

(PDT) either act also as fluorescent labels for imaging or a multi-functional nanomaterial was prepared by combining different building blocks, including drug molecules and fluorophores. A GO based drug delivery system was reported by Zhou and Jiang in 2011.[188] The PDT photosensitizer hypocrellin A (HA) was non-covalently immobilized on the GO surface and it was found that HA / GO was still able to generate singlet oxygen upon illumination. The intrinsic fluorescence of HA allowed for biological imaging and the authors could confirm cellular uptake of HA / GO by HeLa cells. Illumination of the cells incubated with HA / GO confirmed a significant photoinduced cytotoxicity, while in the dark the cells showed a high viability. In a recent follow-up study, the authors co-loaded the HA / GO nanomaterial with the chemotherapy drug SN-38, combining chemotherapy with PDT – See Figure 9.[189] Again, for cellular imaging the fluorescence of HA was exploited, clearly indicating cellular uptake in the cytoplasm of the studied A549 cells. The combination of both drugs led to a significant increase of the anticancer efficiency, compared to reference GO systems including just one drug on the GO. Cui and co-workers published another approach for the delivery of PDT agents.[190] The photosensitizer Chlorin e6 (Ce6), a porphyrinoid, was immobilized onto the surface of GO *via* non-covalent functionalization. Additional targeting was accomplished by the introduction of folic acid. The fluorescence of the Ce6, even though it was partially quenched upon attachment to the GO, was sufficient for cellular imaging and confirmed the internalization of the folic acid-GO / Ce6 nanomaterial by the investigated MGC803 human stomach cancer cells. In addition, the phototoxicity of the nanomaterial was proven, with a 90 % loss of cell viability upon illumination. The photosensitizer Ce6 was used by the group of Liu as well, also non-covalently attached to the surface of PEGylated GO.[191] KB cells readily internalized the PEG-GO / Ce6 nanomaterial, what was verified by confocal microscopy utilizing the intrinsic fluorescence of Ce6. A significant phototoxicity was observed upon laser illumination at 660 nm, but not upon illumination at 808 nm. However, if the cells were illuminated with a laser at 808 nm before the PDT treatment with 660 nm laser light, the mild photothermal heating of the GO led, most likely, to a desorption of the Ce6 from the GO surface inside the cells. This increased the efficiency of the PDT largely and also resulted in an increase of the fluorescence intensity inside the cells, which was again observed by confocal microscopy – See Figure 10. Another porphyrinoid photosensitizer used in drug delivery systems based on graphene was HPPH, also known as Photochlor®.[192] HPPH was loaded on PEGylated GO by means of non-covalent functionalization, similar to the examples illustrated. *In vitro* studies on 4T1 murine breast cancer cells showed that PEG-GO / HPPH was readily internalized. Although the fluorescence of HPPH was significantly quenched upon attachment to the GO, the intensity was still high enough for cellular imaging. PDT studies showed an efficient therapeutic effect upon illumination. For *in vivo* studies, the authors injected the PEG-GO / HPPH in 4T1 tumour bearing mice and could observe strong fluorescence inside the tumours, indicating a high uptake of PEG-GO / HPPH. Metallation of HPPH with ^{64}Cu allowed for PET imaging, which supported the results from fluorescence imaging. The accumulation of the photosensitizer system inside the tumours led to a large improvement of the PDT efficiency *in vivo*, upon laser illumination at 671 nm, rendering this approach as highly promising for future cancer therapy.

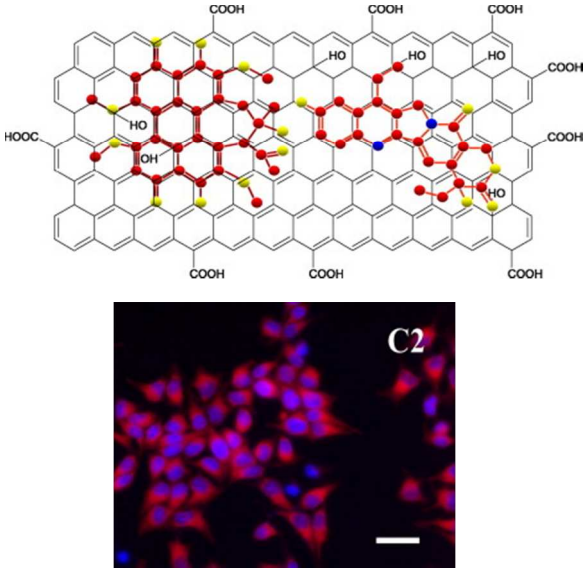

Fig. 9 Schematic representation of the SN-38 and HA co-loaded GO (top). Fluorescence microscope image of A549 cells incubated with SN-38 and HA co-loaded GO. Blue fluorescence – Hoechst 33342 nucleus stain, red fluorescence – HA. Reprinted from Ref. 189, copyright (2014), with permission from Elsevier.

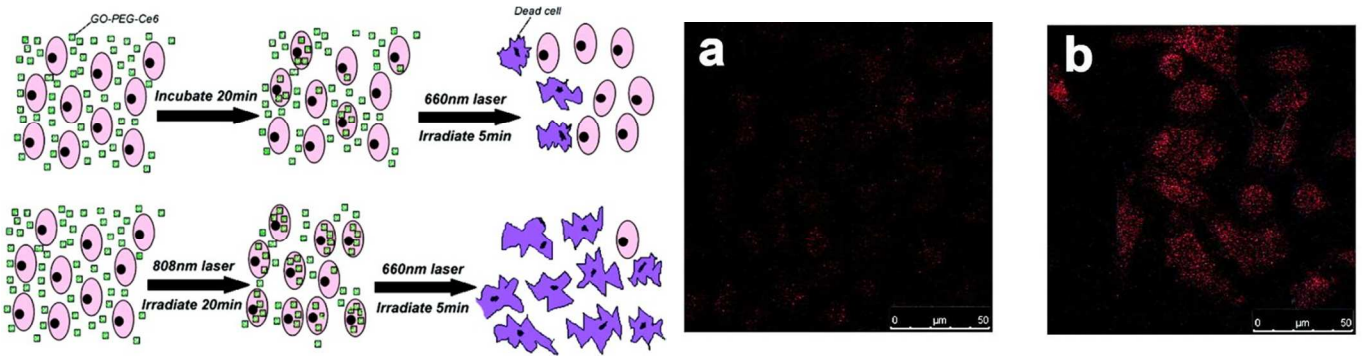

Fig. 10 Schematic representation of the photothermally enhanced efficiency of the PDT upon illumination with a laser at 808 nm (left). Confocal images of KB cells incubated with PEG-GO / Ce6 without (a) and with (b) irradiation with a laser at 808 nm. Reprinted with permission from Ref. 191. Copyright (2011) American Chemical Society.

The group of Wang reported functionalization of RGO with gold nanoclusters (GNC) with sizes ranging from 2 – 3 nm.[193] The GNC / RGO nanomaterial was internalized by the tested HepG2 cells and the fluorescence of the GNCs allowed for cellular imaging by laser confocal microscopy. Additional drug delivery was accomplished by the non-covalent functionalization of the GNC / RGO material with DOX. The use of RGO as drug carrier largely increased the anti-cancer efficiency of DOX.

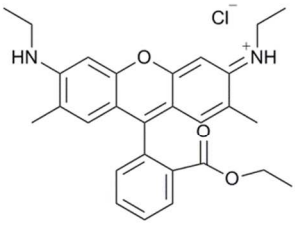

Rhodamine 6G

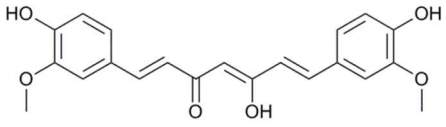

Curcumin

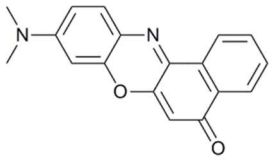

Nile Red

Biomaterials such as gelatine were used by Liu *et al.* to prepare water-soluble, biocompatible graphene nanomaterials.[194] This graphene derivative was employed as carrier for either fluorescent dyes for biological imaging, here rhodamine 6G, or DOX as chemotherapeutic agent. The nanomaterial was uptaken by the investigated MCF-7 cells and the fluorescence of the rhodamine 6G derivatives was suitable for cellular imaging. In a very recent study, Maity *et al.* coated colloidal graphene with carbohydrates and attached folic acid as targeting moiety.[195] The carbohydrates employed were chitosan in combination with dextran or fluorescein-functionalized dextran. The latter allowed for cellular imaging in control experiments. In addition, the authors loaded the graphene nanomaterial *via* non-covalent functionalization with a variety of different drugs and also fluorophores such as curcumin, paclitaxel, camptothecin, DOX and nile red. Nile red was used as reference fluorescence dye for imaging, but also curcumin and DOX showed fluorescence suitable for cellular imaging after being released from the graphene carrier material. Bound to the graphene, their fluorescence signal was largely quenched. The group of Park presented an approach for a drug delivery nanoplatform with temperature and pH-tuneable fluorescence, prepared from GO and a BODIPY-polymer conjugate.[196] Notably, at lysosomal pH, the BODIPY dye emitted a bright fluorescence, while at physiological pH no fluorescence was observed. The cellular uptake of the nanomaterial by MDA-MB 231 breast cancer cells was studied, together with the delivery of DOX as chemotherapeutic drug. In a recent follow-up study, the authors included a photoswitchable spiropyran dye in the multifunctional nanoplatform leading to multicolour stimuli-responsive fluorescent nanoparticles.[197] Biological imaging was studied on A549 cells and *in vivo* on Balb/c mice. Dai and co-workers carried out a study using a photothermal therapeutic approach.[198] Nanosized RGO was functionalized non-covalently by PEG bound amphiphilic polymers, cyanine dye 5 (Cy5) was attached as fluorescent tag for imaging purposes. An Arg-Gly-Asp peptide was crafted to the RGO as targeting moiety. Cellular uptake by U87MG cells was verified by confocal microscopy. Irradiation with NIR light caused a selective photothermal ablation of the tumour cells, while without NIR irradiation, the RGO nanomaterial showed just slight cytotoxicity in relevant concentrations.

Fluorescently Labelled Carbon Nanohorns

SWCNHs are not widely employed in biological imaging, but a few studies are published. In an early report, Zhang *et al.* investigated Zn-phthalocyanine (ZnPc) functionalized, protein crafted SWCNHs for the combined photodynamic and hyperthermic phototherapy of cancer.[199] Oxidized SWCNH were

loaded in a first step with ZnPc and then covalently functionalized with BSA. The autofluorescence of BSA was detected in 5RP7 cells (transformed rat fibroblasts) and combined photodynamic and hyperthermal therapy led to damage and destruction of the cells upon laser irradiation at 670 nm. Also *in vivo* experiments with mice revealed a combined photodynamic and hyperthermal destruction of tumours with the presented SWCNH / ZnPc- BSA nanomaterial. In 2010, Dorn and collaborators prepared double-functionalized SWCNHs. Encapsulated $Gd_3N@C_{80}$ or $Lu_3N@C_{80}$ allowed for MRI or X-ray imaging, while ZnS-capped CdSe quantum dots were used as fluorescent imaging agents.[200] Another approach was presented by the group of Xu, which reported a nanocomposite made of SWCNHs and $NaYF_4$:Yb,Er upconversion luminescent nanoparticles.[201] The composite was formed through covalent bonding between carboxylic acid groups on the SWCNHs and the amine groups of the nanoparticles. Further covalent functionalization of the composite with rabbit anti-CEA8 antibodies resulted in the efficient internalization by HeLa cells. Upconverted fluorescence emission (excitation at 980 nm, emission at 540 nm) was observed inside the cells.

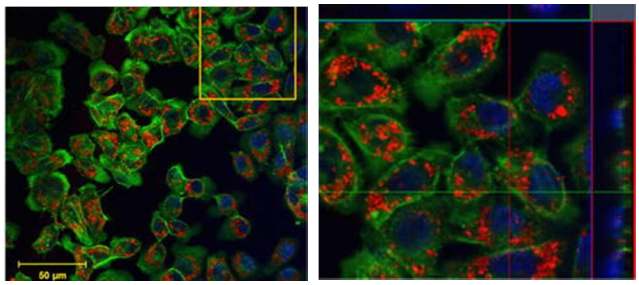

Fig. 11 Images illustrating the cellular uptake of CdSe/ZnS functionalized SWCNHs by AY-27 cells (left). Magnification of the area indicated by the yellow box (right). Green fluorescence – Oregon Green©, blue fluorescence – DAPI nuclear stain, red fluorescence – SWCNH-QD conjugates. Adapted from Ref. 202 with kind permission from Springer Science and Business Media.

The combination of quantum dots with SWCNHs was investigated in two very recent studies.[202,203] The earlier study reports the functionalization of SWCNHs with CdSe/ZnS core/shell nanoparticles and their uptake by several malignant cell lines – See Figure 11 for an example.[202] The cellular distribution of SWCNH-QD conjugates was studies in U-87 MG (glioblastoma), MDA-MB-231 (breast cancer) and AY-27 (bladder transition cell carcinoma) cells. In addition, cytotoxicity studies were carried out. In the latter report, SWCNHs were functionalized in the first step with chitosan and then subsequently with CdTe QDs, which were attached to the SWCNH/chitosan nanocomposite.[203] The functionalized SWCNHs were successfully probed *in vitro* for the imaging of HeLa cells as well as *in vivo* for the imaging of *Caenorhabditis elegans.*

Intrinsic Fluorescence Features of CNMs utilized for Imaging

Fluorescent Carbon Nanotubes

Fluorescent CNTs have been widely studied as *in vitro* and *in vivo* imaging agents. The first report, where NIR emitting SWCNTs were employed for cellular imaging dates back to 2004, when Weisman and collaborators incubated macrophage cells with SWCNTs.[74] The SWCNT NIR emission remained intact upon cellular uptake, but underwent a slight bathochromic shift. This study rendered the microscopic detection of fluorescent SWCNTs inside of cells as a powerful method to investigate the interactions of CNTs with cells. Strano and collaborators studied the cellular uptake of DNA wrapped SWCNTs by 3T3 and myoblast stem cells by exploiting the CNTs' NIR fluorescence.[75]

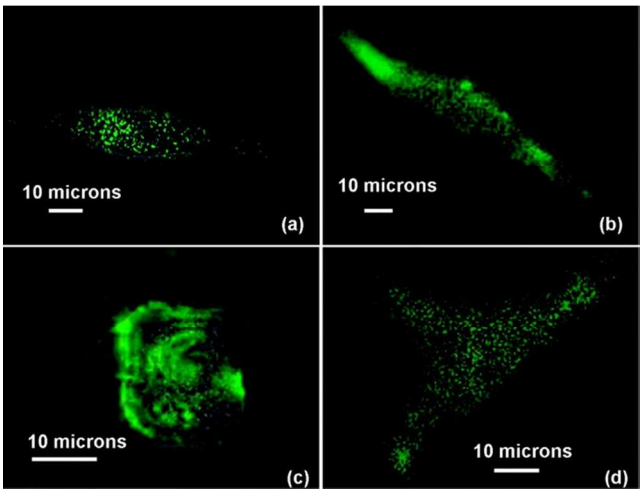

Fig. 12 Localization of length-sorted sodium deoxycholate coated SWCNTs in cells Length of the SWCNTs: (a) 660 ± 40, (b) 430 ± 35, (c) 320 ± 30, and (d) 130 ± 18 nm. Reprinted with permission from Ref. 207. Copyright (2009) American Chemical Society.

Complimentary Raman imaging was carried out and transmission electron microscopy (TEM) revealed the presence of SWCNTs inside cytoplasmic vesicles in the perinuclear region of the cell. While most studies focus on the NIR fluorescence of semiconducting SWCNTs, also the SWCNT centred fluorescence in the visible region[86,87,88] was studied by Lacerda *et. al* to follow the intracellular trafficking of SWCNTs in A549 cells.[204] It was found, that the coating of the CNTs or any other kind of extensive CNT functionalization did not alter the intracellular trafficking. In general, the authors conclude that the SWCNTs accumulate in the perinuclear region of the cell, corroborating earlier results. The group of Dai reported the utilization of NIR emitting, PEGylated SWCNTs, which were conjugated to Rituxan antibodies for the recognition and imaging of Raji cells (B cell lymphoma).[205] Other cells, lacking the antibody specific CD20 cell surface receptors were not visible under the fluorescence microscope. Also the targeting and imaging of BT-474 cells with Herceptin-SWCNT conjugates was successfully demonstrated in this study. MCF-7 cells lacking the HER2/neu cell surface receptor for Herceptin were used as negative probe. This study demonstrated impressively the possibility to target cells with specific surface receptors by using antibody functionalized SWCNTs and utilize the CNTs' intrinsic fluorescence for imaging. In another study from 2008, Jin *et al.* utilized the fluorescence of SWCNTs to track the endocytosis, intracellular trafficking, and exocytosis of SWCNTs in NIH-3T3 cells,

generating trajectories of the motion of SWCNTs in biological samples.[206] In a follow-up study, the cellular uptake and expulsion rates of length-fractioned SWCNTs were investigated in NIH-3T3 cells and a quantitative model for the correlation of the endocytosis rate with the nanoparticle geometry was developed.[207] Again, the tracking of the intrinsic SWCNT fluorescence inside the cells was utilized for this purpose – See Figure 12. The SWCNT NIR fluorescence was also used to identify SWCNTs in the liver tissue of rabbits, in a study investigating the mammalian pharmacokinetics of SWCNTs.[208]

In a first *in vivo* study, larvae of *Drosophila melanogaster* were fed with SWCNT containing food.[209] The NIR fluorescence signal could be detected in the living larvae and was used for imaging. By identifying individual SWCNTs in the tissue of dissected specimens, the biodistribution of the SWCNTs was determined. No short-term toxic effects, impaired growth or changes in the viability of the *Drosophila* larvae were detected, neither were effects on the fertility of the mature individuals observed. A first *in vivo* study on mice, in combination with initial *in vitro* experiments, was published in 2009 by the group of Dai, utilizing different kinds of NIR fluorescent phospholipid-PEG coated SWNTs.[210] For targeted cell imaging, an Arg-Gly-Asp peptide was attached to the SWCNTs and the selectivity for the $\alpha_v\beta_3$-integrin positive cell U87 MG cell line was proven. *In vivo* studies were carried out with nude mice and tumour bearing LS174T mice. After injection in nude mice, NIR fluorescence imaging revealed that the phospholipid-PEG coated SWCNTs gave bright images with a good contrast. The SWCNTs could be identified in the vasculature under the skin and also in deeper organs such as liver and spleen. With time, the SWCNTs were cleared from the body. For the imaging of blood vessels in tumours of living mice, a relatively high dose of phospholipid-PEG SWCNTs was injected in LS174T mice. By taking high-magnification (50x) images up to 90 minutes after the injection, small vessels in a few micrometre resolution were observed. This study clearly demonstrated the ability of SWCNTs to act as NIR fluorophores for the deep-tissue imaging of whole animals *in vivo*. The same research group used comparably functionalized SWCNTs in a follow-up *in vivo* study.[211] The SWCNTs were utilized as NIR tumour imaging agents and also as absorbers for photothermal tumour ablation, upon irradiation with a NIR laser. The photothermal treatment of the tumours turned out to be highly efficient and the high SWCNT uptake of the tumours allowed for the acquisition of bright images. Even more advanced *in vivo* imaging of mice was reported by the same authors in 2011.[79] High frame-rate video imaging of the SWCNT NIR fluorescence enabled the authors to follow the SWCNT circulation in the blood stream in real-time through the lungs and kidneys. Later, the presence of SWCNTs in the spleen and liver was observed. By altering the polymer used for coating the SWCNTs, their uptake by the tumours could be increased and allowed for a more detailed, *in vivo* video-rate tumour imaging – See Figure 13.[212] The use of chirality enriched SWCNTs, in subsequent work, further improved the *in vivo* imaging of mice.[213] The (12,1) and (11,3) SWCNT enriched samples showed a 5x higher photoluminescence upon excitation at 808 nm than unsorted SWCNTs. Consequently the dose of the injected SWCNTs could be significantly lowered and still, bright SWCNT NIR fluorescence suitable for real-time video imaging was observed. The concept was further extended to photothermal tumour ablation employing chirality enriched (6,5) SWCNTs.[214] As expected the dose of injected enriched SWCNTs could be significantly lowered, compared to as-produced SWCNTs. The efficiency of the photothermal tumour ablation remained excellent and the SWCNT NIR fluorescence allowed obtaining bright images of the tumour tissue *in vivo*. In another report, the blood flow in the hind limb of mice was studied.[215] The imaging of the SWCNT NIR fluorescence enabled the authors to follow the distribution of SWCNTs in the blood stream and led to detailed images of the vascular system. To a depth of 1-3 mm, the high spatial and temporal resolution of this technique allowed for the quantification of the blood velocity in normal and femoral arteries. Yi *et al.* reported another approach for deep tissue *in vivo* imaging.[216] The authors utilized genetically engineered multi-functional M13 phage to assemble SWCNTs and ligands for the targeted imaging of tumours. The imaging was accomplished by using the SWCNT-M13 phage-based material in low concentrations, no toxic effects were reported.

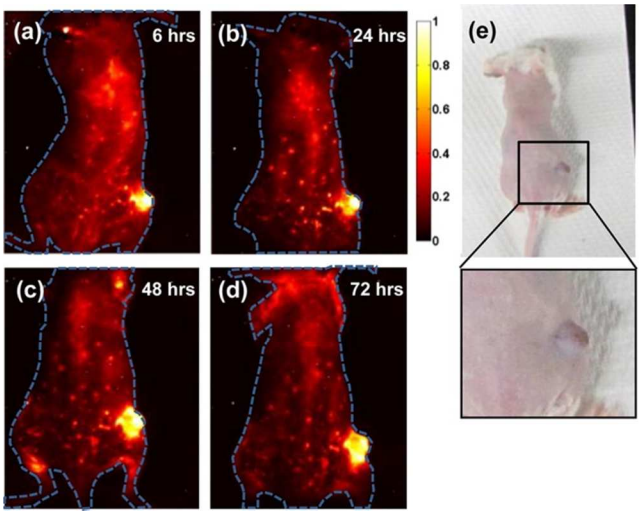

Fig. 13 NIR-II imaging of xenograft 4T1 tumour with high uptake of SWNTs. (a–d) Time course NIR-II fluorescence images of the same mouse injected with coated SWCNTs, showing increasing tumour contrast due to the accumulation of nanotubes inside the tumour. (e) Digital camera image of the same mouse as shown in (a–d), with noticeable darkening of the tumour due to the high tumour uptake of SWNTs. Reprinted with permission from Ref. 212. Copyright (2012) American Chemical Society.

In addition to mice, which were the subject of all of the previously mentioned *in vivo* studies, also fishes (*e.g.* fathead minnows, *Pimephales promelas*) were studied.[217] Observation of the SWCNTs' NIR fluorescence allowed for the tracking of SWCNTs in the fish after gavage of aqueous pristine SWCNT / gum arabic suspensions. SWCNT fluorescence was detected in the gastrointestinal system and not in other tissues, suggesting that SWCNTs were not intestinally absorbed.

Graphene Quantum Dots and Related Nanomaterials

Fluorescent GQDs / CDs are widely applied for biological imaging.[218] Early work dates back to 2011, when Zhu *et al.* reported the synthesis of GQDs by a hydrothermal method from

GO,[219] a method that was applied for the synthesis of a large variety of GQDs / CDs discussed in this section. The GQDs were reported to have a fluorescence quantum yield as high as 0.11, showed excitation-dependent as well as solvent-dependent fluorescence in the visible region and were water-soluble. This enabled for fluorescence imaging of MG-63 cells, which showed a good viability upon incubation with GQDs. Furthermore, it was demonstrated that the excitation wavelength dependent fluorescence emission of GQDs could also be observed after being internalized in cells. In another report, GO based, very small (1.5 – 5.0 nm) GQDs were used for the imaging of HeLa cells with results comparable to the previous study.[220]

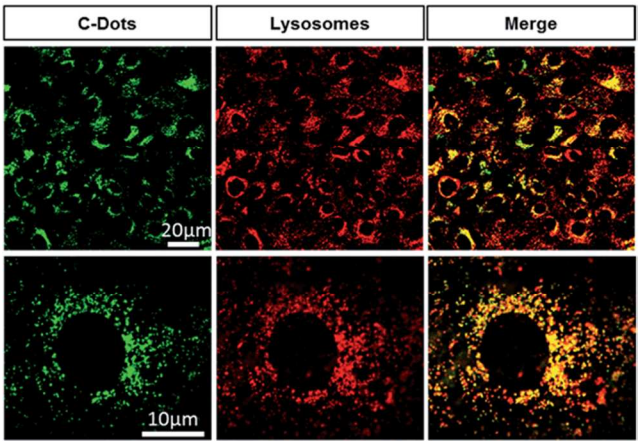

Fig. 14 Representative confocal images of MCF-7 cells incubated for 48 hours with CDs. The upper panels display a large field of view with several cells, while the lower panels focus on a single cell. Green fluorescence – CDs, red fluorescence – Lysotracker Red. Reproduced from Ref. 232 with permission from The Royal Society of Chemistry.

The methods for the fabrication of GQDs vary, especially by using different carbonaceous starting materials. Dong *et al.* for example utilized Vulcan CX-72 carbon black for the preparation of GQDs.[221] The authors probed the GQDs for the imaging of MCF-7 cells with good results. Also carbon fibres were used for the fabrication of GQDs.[222] The authors were able to vary the size of the as-prepared GQDs and thus control the emission colour and the band gap. In biological experiments, the GQDs were found to be suitable for the imaging of T47D cells and showed a low cytotoxicity. The group of Yang presented another approach.[223] In a first step, polymer-like CDs were prepared from citric acid and ethylenediamine, which were then converted in a hydrothermal reaction to CDs. These CDs showed a bright excitation wavelength dependent fluorescence with fluorescence quantum yields as high as 0.80. The authors tested the CDs in several applications, including the imaging of MC3T3 cells. Yellow-emitting GQDs were reported by Zhang *et al.*, who prepared the GQDs by the electrolysis of graphite rod anodes in NaOH followed by reduction with hydrazine.[224] Cellular imaging was probed with three kinds of stem cells (neurosphere cells, pancreas progenitor cells and cardiac progenitor cells). Confocal fluorescence microscopy revealed cellular uptake of the GQDs, which could be identified in the cytoplasm of the cells. In another study, the groups of Tao and Wang reported the synthesis of fluorescent nanographite oxides in different sizes, prepared from graphite powder in a hydrothermal reaction.[225] The nanomaterial showed size-dependent fluorescence and the authors could isolate several fractions of particles with molecular weights ranging from 1000-3500 Da (green fluorescence), 3500-7000 Da (yellow fluorescence) and >7000 Da (red fluorescence). The nanographite oxide particles were readily uptaken by A549 cells and were observed in the cells' cytoplasm without exhibiting notable cytotoxicity. A method to increase the fluorescence quantum yield of GQDs was reported by Sun *et al.*.[226] Photoreduction of GQDs with isopropanol led to an increase in the GQDs' fluorescence quantum yield by a factor of 3.7 from 0.024 to 0.088. This increased fluorescence intensity resulted in significantly brighter images of A549 cells and also the cytotoxicity of the modified GQDs was reduced. In 2014, a large number of high quality studies on the preparation of CDs and GQDs and their application for cellular imaging were published. In most cases, the CDs were synthesized by hydrothermal one-pot protocols from different organic starting materials as carbon sources. Leading examples include the preparation of CDs from formaldehyde[227] and folic acid[228]. Both studies report the application of the as-prepared CDs as fluorescent agents for the imaging of mouse prosteoblasts[227] and HL-60 cells,[228] respectively. Feng and collaborators reported a green hydrothermal approach for the preparation of amorphous CDs from waste paper.[229] The emission wavelengths of the CDs shifted dependent on the excitation wavelength, an effect that was preserved upon internalization by S180 sarcoma cells. A variation of the classical hydrothermal method was presented in two other reports, which describe the use of microwave irradiation for the synthesis of CDs suitable for cellular imaging. In the first study, the group of Yan utilized ascorbic acid (as carbon source) for the preparation of small diameter (~3.1 nm) CDs and investigated their cellular uptake by Bcap-37 and Hs-587 cells.[230] In the other report, Gu and collaborators prepared CDs from sucrose in diethylene glycol in a microwave reactor.[231] The diethylene glycol CDs were uptaken by C6 glioma cells, which was confirmed by fluorescence microscopy and showed just a low cytotoxicity. The group of Pompa demonstrated super-resolution imaging utilizing biocompatible CDs.[232] Toward this, CDs with diameters of approx. 5 nm were prepared by the laser ablation of a carbon target. MCF-7 cells, incubated with these CDs were investigated by confocal and *ST*imulated *E*mission *D*epletion (STED) microscopy of living and fixed cells. The localization of the CDs in the lysosomes of the cells was observed by co-staining with Lysotracker Red and a high cellular uptake of the non-toxic CDs was verified – See Figure 14.

A CNM related to CDs are hollow carbon nanoparticles (HC-NPs), which were derived from acetic acid and P_2O_5 and subsequently separated by HPLC, yielding several fractions of NPs in sizes between 6.13 and 8.66 nm.[233] Each HPLC fraction of HC-NPs showed different fluorescence features with very distinct emission properties. The various fractions of HC-NPs were probed for cellular imaging of MCF-7 cells with promising results and did not reveal notable cytotoxicity.

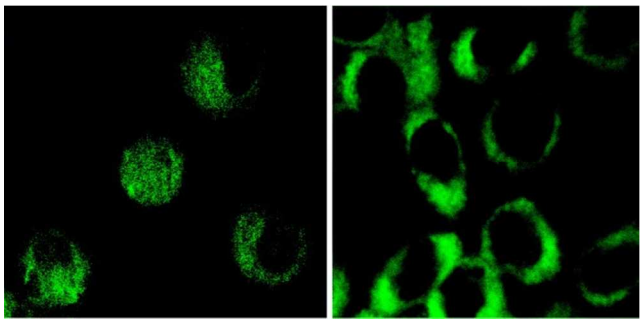

Fig. 15 Representative two-photon luminescence image (800 nm excitation) of human breast cancer MCF-7 cells with internalized CDs. Reprinted with permission from Ref. 212. Copyright (2007) American Chemical Society.

Boron doped GQDs (B-GQDs) were prepared by the electrolysis of graphite rods in an aqueous borax solution.[234] The presence of boron was confirmed by X-ray photoelectron spectroscopy (XPS) and the B-GQDs had diameters between 3-7 nm and a thickness of approx. 1 nm. To probe B-GQDs as agents for fluorescence imaging, HeLa cells were incubated with the B-GQDs and the cellular uptake was followed by confocal microscopy revealing the translocation through the cell membrane by bright yellow fluorescence emission inside the cells. In addition, a low cytotoxicity was observed.

CDs are also applicable for multi-photon bioimaging. A first report dates back to 2007, where the group of Sun observed one and two-photon fluorescence in CDs upon excitation with a 458 nm laser or a femtosecond pulsed laser at 800 nm, respectively.[235] The green two-photon luminescence was also observed, when the CDs were internalized by MCF-7 cells following excitation with the pulsed 800 nm laser – See Figure 15. In another report, Wang and Gu reported two-photon cellular imaging using GO nanoparticles.[236] For therapeutic applications, transferrin was immobilized on the GO nanoparticles as targeting moiety for transferrin receptor overexpressing cancer cells. The cellular uptake of the GO nanoparticles was verified by fluorescence microscopy of the yellow two-photon luminescence signal upon laser excitation at 790 nm, leading to bright images of the cells. Also GQDs were successfully used for two-photon up-conversion cellular imaging of mouse osteoblastic cells.[237] The group of Tian presented a CD based two-photon fluorescent imaging agent.[238] Interestingly, the fluorescence probe allowed for the imaging and biosensing of pH gradients (in a range between 6.0 – 7.5) in living cells and tissues. Human A549 cells, mouse LLC-MK2 cells and tumour tissue from nude mice were investigated and a bright two-photon fluorescence signal was observed upon excitation at 800 nm.

A few examples of *in vivo* imaging, using CDs as imaging agents, are published. In one report, the group of Sun studied the performance of PEGylated CDs and CDs doped with ZnS.[239] The CDs revealed fluorescence quantum yields of 40% and 60%, respectively. Female DBA/1 mice were used to study *in vivo* imaging following two injection modes (subcutaneous and front extremity). The fluorescence signal of both investigated CDs was observed subcutaneous following injection. Also intradermally injected CDs in the front extremities could be visualized by optical fluorescence microscopy, rendering CDs as potential imaging agents for future *in vivo* studies and biomedical applications. The non-invasive imaging of gliomas in the brain of mice was reported recently by Ruan *et al.*.[240] *In vitro* experiments confirmed the cellular uptake of CDs with a diameters of approx. 5 nm by C6 glioma cells. In subsequent *in vivo* studies, nude mice bearing glioma in the brain were injected through the tail vein with CDs. The accumulation of fluorescent CDs was observed inside the glioma in the brain already minutes after the injection, followed by a rapid systemic elimination. *Ex vivo* studies were carried out to elucidate the fate of the CDs in different body tissues. The two-photon luminescence of PEGylated GO nanoparticles was utilized by He and collaborators for *in vivo* functional bioimaging, following initial *in vitro* studies.[241] One hour after intravenous injection of the PEG-GO, the authors observed bright two-photon fluorescence in the ear blood vessels of mice. Also in the brain of the mouse, microinjected PEG-GO nanoparticles were observed, down to a depth of 300 μm, following excitation with a femtosecond pulsed laser at 810 nm.

Nanodiamonds

NDs as fluorescent probes for imaging have been used for cellular imaging already for some time;[242] however, the recent years have witnessed tremendous progress in this field. The emission wavelength of NDs is thereby located in the visible region, with characteristic green to red emission between 550 and 800 nm.[243]

An early report dates back to 2005 and was published by Chang and collaborators, who reported the application of fluorescent NDs as non-bleaching imaging agents for human 293T kidney cells with no observed cytotoxicity.[244] After this initial work, the same authors characterized two different kinds of fluorescent NDs with average sizes of 35 and 100 nm and studied their cellular uptake by HeLa cells with promising results, which signalled the huge potential of NDs as high quality imaging agents.[243] Also the imaging of A549 human lung epithelial cells and *Escherichia coli* was investigated.[245] The authors concluded, that fluorescent NDs are useful probes for the detection of interactions between NDs and cells / bacteria. NDs, with diameters of about 25 nm, prepared by a novel, large-scale synthetic method, were investigated for the fluorescence imaging of live HeLa cells with excellent results.[23] The cellular uptake of NDs by HeLa cells was also the content of a report from 2008, which examined the NDs' internalization pathway and localization inside the cell.[246] This study revealed that, following internalization, the fluorescent NDs were not trapped in endosomes, which is highly advantageous for potential drug delivery applications. In consecutive work, the uptake mechanism of NDs in HeLa was further studied by blocking selectively different uptake pathways.[247] It was found that NDs entered the cells mainly by endocytosis, but also on a clathrin-mediated pathway. While larger ND nanoparticles as well as aggregates localized in vesicles, small ND particles appeared to be in the cytoplasm. The proposed cellular uptake mechanisms were later corroborated by the group of Cheng, who studied the internalization of NDs by different cancer and non-cancer cells.[248] Cancer cells, however, revealed a higher uptake of NDs.

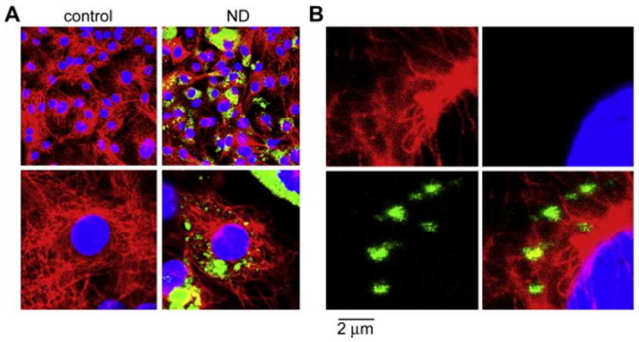

Fig. 16 Fluorescence microscopy images of the ND nanoparticle distribution in 3T3-L1 cells. (A) After treatment with or without 100 nm ND particles. (B) Several single ND's clusters were formed and located in cytoplasm but not nucleus. Red fluorescence – microtubule proteins of the cytoskeleton, blue – Hoechst 33258 nuclear stain, green – NDs. Reprinted from Ref. 251, copyright (2009), with permission from Elsevier.

A targeted approach for the imaging of transferrin receptor over-expressing HeLa cells with transferrin bearing NDs was reported by Weng *et al.*.[249] The transferrin NDs were uptaken by the HeLa cells and control experiments confirmed an effective targeting of the transferrin receptors. An approach for targeting mitochondria in cells with fluorescent NDs was presented by Opitz and collaborators.[250] Carboxylated NDs were decorated with either mitochondria or actin targeting antibodies before incubation. The efficiency for targeting the mitochondria was confirmed by fluorescence microscopy rendering NDs promising fluorescent probes for intracellular assays. The effects of 100 nm diameter carboxylated NDs on cell division and differentiation was reported by Liu *et al.*.[251] Both, A549 lung cancer cells and 3T3-L1 embryonic fibroblasts internalized the ND particles. Long-term experiments did not show any cytotoxic effects and the cell cycle was not affected. The intense fluorescence of the NDs resulted in bright images of the living cells during cytokinesis – See Figure 16. A further detailed study on the short-term and long-term exocytosis of NDs in various cell lines was reported in 2011.[252] The excellent applicability of NDs as long-term cell tracker was highlighted and the imaging of ND labelled cells over several days was accomplished. Super-resolution cellular imaging of fluorescent NDs, using a STED microscope, was presented by Tzeng *et al.*.[253] Carboxylated NDs were solubilized *via* non-covalent functionalization with BSA α-lactalbumin to prevent agglomeration. Uniform cell labelling was illustrated and super-resolution pictures of ND labelled HeLa cells were obtained. Chiang and collaborators studied the cellular uptake and toxicology of fluorescent NDs with different surface functionalities such as carboxylic acids, transferrins and amino-silanes by HeLa.[254] Again, transferrin targeting was proven to be effective. However, illumination of transferrin-NDs exposed cells revealed a certain phototoxicity, induced by the functionalized NDs when compared to untreated cells. This paves the way to future theranostic ND based nanomaterials combining imaging with the photokilling of malicious cells. Further studies included the revelation of the influence of the presence of NDs on the oxidation states of human red blood cells.[255] By using a variety of techniques, including laser scanning fluorescence microscopy, it was shown that NDs do neither cause haemolysis nor effect the blood cells' viability or the oxygenation / deoxygenation processes. This renders NDs excellent biological fluorescent probes for imaging, without causing problems with the investigated organisms' blood physiology. Also important for medical applications is the imaging of the self-renewal and differentiation of stem cells. In a recent research article, Wu *et al.* studied the fate of type I and II pneumocytes on a long-term timescale after transplantation, by labelling the cells with fluorescent NDs.[256]

In addition to surface functionalized NDs of different sizes, some other approaches for using NDs as fluorescent probes were reported. One leading example includes the use of fluorescent, iron nanoparticle bearing magnetic NDs, which were successfully employed for the separation, tracking and fluorescence imaging of various types of cancer cells by the group of Chao.[257] In a very recent study, Rehor *et al.* reported the coating of fluorescent NDs with translucent, biocompatible silica shells.[258] The silica shell did not alter the fluorescence of the NDs and further modification with PEG led to highly stable ND solutions. The modified NDs showed superior cellular uptake and translocation, compared to pristine NDs. Additional surface functionalization with molecules and bio-molecules as vectors was reported as well. In a very recent follow-up study, the targeted delivery of fluorescent, multi-functionalized NDs was presented.[259] Slegerova *et al.* coated fluorescent NDs firstly with a biocompatible polyacrylamide shell and then immobilized the commercial dye Alexa Fluor 488™ next to a peptide, which targets selectively the $\alpha_v\beta_3$ receptors on glioblastoma cells, on the nanoparticles. The cellular uptake of the NDs was confirmed by confocal fluorescence microscopy utilizing the green fluorescence of the Alexa Fluor dye and the red intrinsic fluorescence of the NDs for two-colour imaging.

Kawata and collaborators presented multi-colour imaging of HeLa cells with green and red emitting fluorescent NDs recently.[260] A direct electron-beam excitation-assisted fluorescence (D-EXA) microscope was used for recording the multi-colour fluorescence images simultaneously and rendered this technique useful for future biological imaging applications.

NDs were also successfully employed as multi-functional delivery platforms for theranostic purposes. The group of Cao and collaborators reported in 2010 the immobilization of the chemotherapeutic drug paclitaxel on small (3-5 nm diameter) NDs.[261] Treatment of A549 lung cancer cells with the paclitaxel NDs showed largely reduced cell viability. The cellular uptake and the induction of defects in the cells, induced by the paclitaxel-NDs, was observed by confocal microscopy The ability of NDs to deliver small interfering RNA (siRNA) into Ewing sarcoma cells was investigated by Alhaddad *et al.*.[262] In a first step, NDs were coated with a cationic polymer and subsequently the siRNA was adsorbed. The cellular uptake and intracellular distribution was studied by confocal microscopy utilizing the intrinsic fluorescence of the NDs and, for co-localization experiments, fluorescein labelled siRNA.

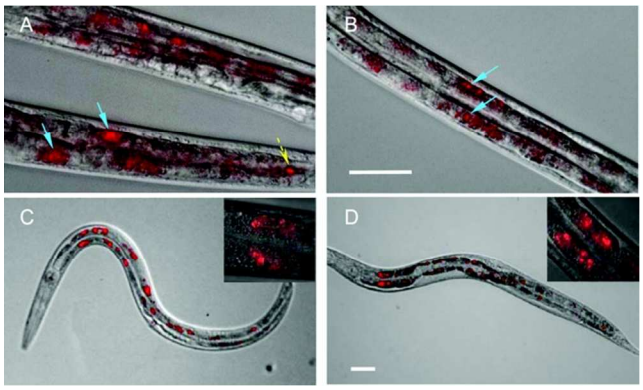

Fig. 17 Epifluorescence/DIC-merged images of wild-type *C. elegans* fed with bioconjugated FNDs. (A, B) Worms fed with dextran-coated FNDs (A) and BSA-coated FNDs (B) for 3 h. FNDs can be seen to be localized within in the intestinal cells (blue solid arrows) and a few stay in the lumen (yellow dash arrow). (C, D) Worms fed with dextran-coated (C) and BSA-coated (D) FNDs for 3 h and recovered on to E. coli bacterial lawns for 1 h. In both cases, the FNDs staying in the lumen are excreted out, whereas the ones localized in the cells retain. Insets: 100× magnified images of the FNDs within the intestinal cells. Anterior is left and dorsal is up in all the figures. Scale bars are 50 μm. Reprinted with permission from Ref. 264. Copyright (2007) American Chemical Society.

A few *in vivo* studies, where NDs were used as fluorescent probes, were reported. In one study, the interaction of two different kinds of NDs (with 5 and 100 nm diameter) with the ciliated eukaryotic unicellular organisms *Paramecium caudatum* and *Tetrahymena thermophile* was studied.[263] The NDs were entering the food vacuoles of the microorganisms and excreted later on. Imaging was accomplished by confocal microscopy. The toxicity of NDs for the observed microorganisms was low, but nevertheless significantly larger than as previously reported for *in vitro* cell cultures. The effects of fluorescent NDs on *C. elegans* were investigated as well.[264] NDs were either fed to the worms or injected into the gonads, what led to a delivery of the NDs to the embryos of the next generation. It turned out, that the non-toxic NDs were ideal agents for imaging the whole digestive system of the worms and allowed for tracking the cellular and developmental processes of the organisms *in vivo* – See Figure 17. The same authors followed up the latter work by utilizing bare and bioconjugated NDs in *C. elegans* and zebrafish.[265] It was found that for both organisms, NDs could be delivered to the embryos of the next generation providing excellent fluorescence properties for *in vivo* imaging. In a study from 2012, Igarashi *et al.* studied the application of fluorescent NDs as imaging probes *in vivo* in *C. elegans* and mice.[266] The authors report, that even in the presence of an intense autofluorescence background, it was possible to obtain images with an excellent contrast. Another study on mice was reported by Cheng and collaborators who investigated the long-term stability and biocompatibility of 100 nm diameter NDs.[267] The fate of the injected fluorescent NDs was investigated by *in vivo* whole body imaging as well by *ex vivo* examination of various body tissues. The authors report no toxic effects of the NDs on the mice, rendering NDs furthermore as promising *in vivo* imaging agents.

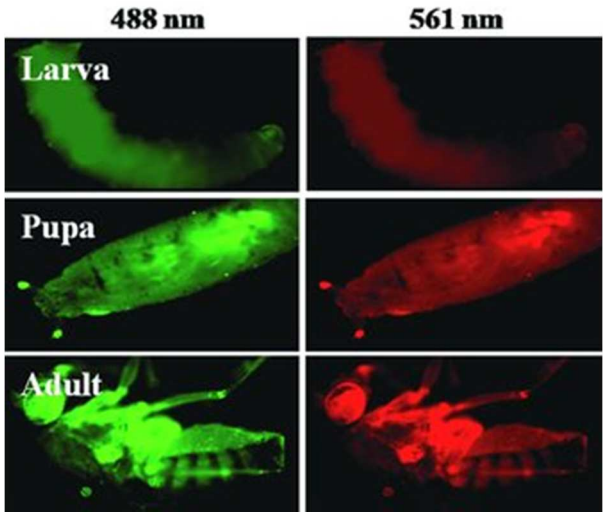

Fig. 18 *D. melanogaster* labelled with fluorescent CNOs under different filters. Reprinted from Ref. 100 with permission from John Wiley and Sons, copyright (2011).

Fluorescent Carbon Nanoonions

The group of Sarkar probed fluorescent CNOs as imaging agents in two consecutive studies.[100,268] In the initial report,[100] the authors utilize CNOs for imaging the full life cycle of *D. melanogaster* – See Figure 18. CNOs were fed to the specimens and the dietary uptake and subsequently the distribution of fluorescent CNOs in the body was visualized by fluorescence microscopy. In the follow-up study,[268] the authors fed CNOs to *E. coli* bacteria, which were then fed to *C. elegans*. For both organisms, the CNO uptake could be visualized by fluorescence microscopy, rendering the fluorescent CNOs as an interesting bioimaging agent, especially since the authors did not observe any toxic effects.

Raman Spectroscopy for Imaging

In the previous section we have discussed the use of intrinsic, and label derived fluorescence of CNMs for imaging. In addition to these fluorescent properties, increasing studies are focused on exploiting the inherent Raman scattering of CNMs for bioimaging. A first study, using CNT Raman scattering for imaging was the aforementioned report by Streller *et al.*, who combined Raman and fluorescence spectroscopy for multimodal cellular imaging.[75] Combined images of SWCNT fluorescence and Raman RBM intensities gave a good impression over the distribution of the SWCNT uptake by the investigated live murine 3T3 cells. The group of Dai published another example for micro-Raman imaging of SWCNTs inside of cells.[269] The authors incubated human T cells with water-soluble PEGylated, siRNA functionalized SWCNTs, which could then be identified inside the cells by their characteristic G-band Raman scattering. The same group also presented multi-colour Raman imaging of live cells, by employing SWCNTs with different ratios of ^{12}C to ^{13}C.[138] Three types of SWCNTs with different isotopic combinations were labelled with different targeting moieties such as Herceptin, Erbitux and RGD-peptide, which target selectively

specific cell-surface receptors – See Figure 19 top. Three cell lines overexpressing the corresponding cell-surface receptors were probed with the functionalized SWCNTs and indeed, the authors showed successfully the selective cell labelling by multi-colour Raman spectroscopy – See Figure 19 bottom. The mapping of the intracellular distribution of CNTs in folate receptor overexpressing T24 (human urinary bladder carcinoma) cells after folate-targeted delivery was reported by Lamprecht *et al.*.[270] The authors utilized the CNTs G-band to visualize the presence of the CNTs in the cell by confocal Raman microscopy. In another study, the labelling of human mesenchymal stem cells with SWCNTs was investigated.[271] The groups of Li and Liu employed PEGylated, proteamine conjugated SWCNTs, which entered the cells readily. Strong Raman scattering was emitted from the SWCNT containing stem cells in vitro. Subsequent *in vivo* studies, where the labelled stem cells were injected into living mice allowed for the detection of a small number of stem cells *in vivo*. In a report from 2012, Wang *et al.* functionalized DNA coated SWCNTs further with noble metal nanoparticles (Ag and Au) and subsequently with PEG.[272] Targeting of KB cancer cells was accomplished by the derivatization with folic acid. Imaging could be accomplished by Raman mapping of the cells, using an IR laser as excitation source. In complementary experiments, the selective photothermal ablation of the SWCNT containing cancer cells was successfully demonstrated by irradiation with a 808 nm laser.

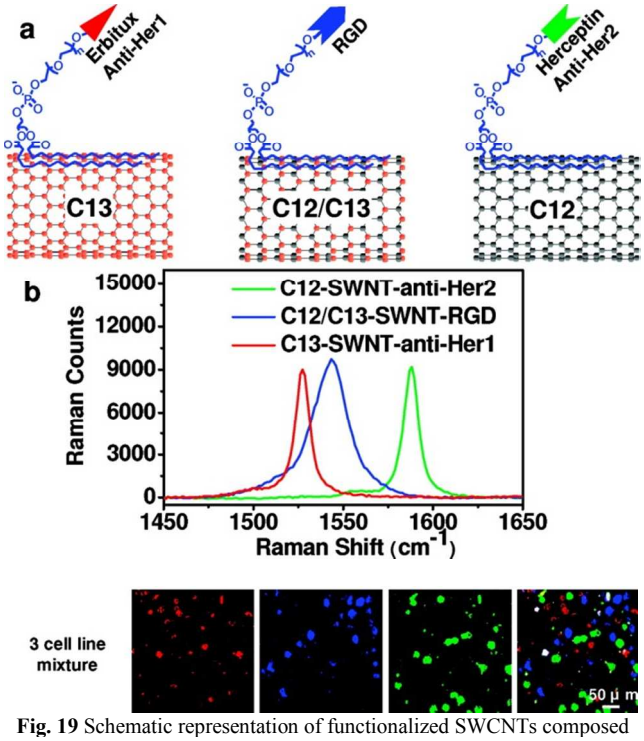

Fig. 19 Schematic representation of functionalized SWCNTs composed of different isotopes (a) revealing different Raman colours (b). Multicolour cellular imaging (bottom). Cells were incubated with a mixture of the three-colour SWCNTs. Reprinted with permission from Ref. 138. Copyright (2007) American Chemical Society.

In biomedical applications, profound knowledge of the distribution of the delivery vectors, and the connected functionalities such as drugs is of great importance. Also the analysis of the efficiency of specific targeting moieties is an essential piece of information for the development and improvement of multi-functional drug delivery systems. A method to monitor the circulation and long-term fate of CNMs, such as CNTs is very helpful. In this context, the work of Hongjie Dai and collaborators on the application of Raman spectroscopy for these purposes deserves closer attention. In an initial study from 2008, PEGylated SWCNTs were injected intravenously into mice and the blood circulation of the SWCNTs was measured *in vivo*, by using the intrinsic Raman features of the CNTs.[273] *Ex vivo* imaging of different tissue samples from the mice gave hints about the distribution of the SWCNTs throughout the organism and also possible excretion pathways. Interestingly, no toxic side effects of the SWCNT treatment were observed in a time-period of 3 months. In subsequent work, the authors immobilized the anti-cancer drug Paclitaxal on PEGylated SWCNTs *via* a cleavable ester bond.[274] The SWCNT-Paclitaxal conjugate showed a higher cytotoxic efficiency against murine 4T1 breast cancer cells and increased tumour growth suppression in tumour bearing BALB/c mice than the free drug molecule. This observation was led back to a prolonged blood circulation and an increased cellular uptake. The biodistribution in the tissue of the mice was determined *ex vivo* by Raman spectroscopy, utilizing the strong Raman G-band signal at 1580 cm^{-1}. The concept of multi-colour Raman imaging, by altering the ^{12}C : ^{13}C isotopic ratios of the applied SWCNTs, was further refined by the use of 5 different SWCNT probes in combination with 5 different targeting moieties.[139] In addition to *in vitro* assays, the various SWCNTs were injected in mice as well and by *ex vivo* Raman imaging, SWCNT labelled tumour cells of different types could be clearly identified. The group of Liu published a therapeutic approach.[275] Different kinds of surface functionalized SWCNTs were injected in mice and the biodistribution of the SWCNTs was determined by Raman spectroscopy. *In vivo* photothermal treatment of tumours in SWCNT treated mice led to a complete destruction of the tumour tissue. The accumulation of SWCNTs in skin tissue could be visualized by *ex vivo* Raman mapping. Also *in vivo* Raman imaging of small animals using SWCNTs as Raman labels was reported.[276] The authors functionalized SWCNTs with a RGD peptide for tumour targeting and injected a sample in the tail-vein of tumour bearing mice. The *in vivo* Raman images revealed an accumulation of the SWCNTs in the tumour tissue and gave rise to further studies on this subject. In subsequent work, the authors could verify the efficiency of the RGD targeting moiety and presented raster-scan Raman images of the tumour area, corroborating the presence of SWCNTs.[277]

NDs were also successfully employed for cellular Raman imaging in some *in vitro* studies. Cheng *et al.* for example demonstrated the surface targeting of growth hormone receptors on A549 cells by using growth hormone functionalized 100 nm diameter NDs.[278] The Raman signal of the NDs was used for confocal Raman mapping and allowed for the verification of the presence of NDs on growth hormone receptors on the cells in high spectral and spatial resolution. The same authors published a study combining fluorescence and Raman imaging to monitor the cellular uptake of NDs by HeLa cells and *E. coli*.[245] In another study by the group of Cheng , the cellular uptake of NDs by A549 lung adenocarcinoma, HFL-1 foetal fibroblast, and Beas-2b human bronchial epithelial cells was investigated by

complementary Raman and fluorescence imaging.[248] Raman mapping turned out to be an excellent method for determining the ND localization in the cell.

Conclusions and Outlook

Carbon nanomaterials have had a tremendous impact in the development of theranostic methods for *in vitro* and *in vivo* biomedical applications, including imaging. Drug delivery and photothermal therapy have been successfully integrated with the targeting of specific cell types, mainly cancer cells. In all these studies, cellular imaging as well as *in vivo* imaging of small animals play an important role in monitoring the internalization of carbonaceous nanovectors by the cells and organisms, and thus the successful delivery of the various functionalities. However, even without additional functionalities, CNMs as agents for fluorescence and Raman imaging allow for exciting insights into the behaviour and function of cells and organisms.

The focus of previous research efforts was on CNTs, NDs and graphene based nanomaterials. However, the future clearly lays in the development of sophisticated, multi-functional theranostic nanomaterials with tailor-made properties for specific purposes. Other CNMs that were not in the centre of previous attention, like CNOs and CNHs, are highly promising for future developments. In addition, other CNMs such as the highly fluorescent cycloparaphenylenes (CPPs)[279,280,281], which were never probed for imaging applications, are of potential interest. With their bright, size-dependent fluorescence emission,[282] CPPs might be a prospective new class of carbon based imaging probes.

The general scope of future developments in biological and medicinal imaging requires the ability to follow the dynamic behaviour structures such as proteins or RNA at single molecular level in living systems. The development of novel nanoprobes for the detection of individual particle level in complex biological environments is thereby a necessity in this context, especially to keep track with the development of super-resolution techniques such as STED.

Acknowledgements

JB and SG are grateful to the Istituto Italiano di Tecnologia (IIT) for funding. SQ is grateful to the University College Dublin for funding.

Cite this: DOI: 10.1039/c0xx00000x

www.rsc.org/xxxxxx

ARTICLE TYPE

Table 1 Comparison of the key features of the presented CNMs

Common Synthetic Methods	Working Wavelength	Sensitivity / Fluorescence Quantum Yield	Toxicity / Biocompatibility
Carbon Nanotubes (Fluorescent Labelled)			
Laser ablation of graphite or different CVD processes followed by purification and covalent and/or non-covalent functionalization of CNTs with fluorophores and additional functionalities.	Dependent on the utilized fluorophore. Excitation and Emission in Vis – NIR I	Highly fluorescent dyes can be applied. Very versatile for *in vitro* imaging.	CNTs reveal toxic effects. Cytotoxicity and a relatively high inflammatory potential was reported in several studies, what can be alleviated by excessive covalent or non-covalent functionalization.
Carbon Nanotubes (Intrinsic Fluorescence)			
Laser ablation of graphite or different CVD processes followed by purification / chemical surface modification.	Excitation: Vis – NIR I; Emission: NIR II	Single CNTs can be detected. Low fluorescence quantum yield (<1%). Deep tissue *in vivo* imaging possible.	CNTs show toxic effects. Non-covalent CNT coating can be applied to reduce these effects. Covalent functionalization eventually reduces the fluorescence quantum yield and is not the method of choice for this particular application.
Carbon Nanotubes (Raman Imaging)			
Laser ablation of graphite or different CVD processes followed by purification / chemical surface modification. Multicolor Raman imaging by isotopic doping.	Not excitation wavelength dependent. Vis – NIR I	Low sensitivity. Deep tissue *in vivo* imaging possible.	CNTs reveal toxic effects. Cytotoxicity and a relatively high inflammatory potential was reported in several studies, what can be alleviated by excessive covalent or non-covalent functionalization. CNT D-band intensity is not significantly affected by functionalization.
Carbon Nanohorns (Fluorescent Labelled)			
Catalyst-free CO_2-laser ablation of graphite.	Dependent on the utilized fluorophore. Excitation and Emission in Vis – NIR I	Highly fluorescent dyes can be applied. A limited number of examples was reported.	Available studies suggest negligible toxicity. Limited data.
Nanodiamonds (Fluorescent Labelled)			
Extraction from detonation soot or high energy treatment of diamond nanocrystallites. followed by chemical modification to introduce fluorophores.	Dependent on the utilized fluorophore. Excitation and Emission in Vis – NIR I	Highly fluorescent dyes can be applied. Multi-colour imaging possible in combination with the intrinsic ND fluorescence.	Available studies suggest negligible toxicity.
Nanodiamonds (Intrinsic Fluorescence)			
Extraction from detonation soot or high energy treatment of diamond nanocrystallites.	Vis	High fluorescence quantum yields were reported. Single diamonds can be detected by high resolution techniques.	Available studies suggest negligible toxicity.
Nanodiamonds (Raman Imaging)			
Extraction from detonation soot or high energy treatment of diamond nanocrystallites.	Vis	NDs could be localized inside the investigated cells.	Available studies suggest negligible toxicity.
Carbon Nanoonions (Fluorescent Labelled)			
Heat treatment of nanodiamonds, arc-discharge of graphite and other methods.	Dependent on the utilized fluorophore. Excitation and Emission in Vis – NIR I	Highly fluorescent dyes can be applied. A limited number of examples was reported.	Available studies suggest mainly low toxicity. Data limited.
Carbon Nanoonions (Intrinsic Fluorescence)			
Pyrolysis of wood wool.	Vis - Excitation wavelength dependent emission	*In vivo* imaging of microorganisms was reported. No high resolution data available.	Available studies suggest low toxicity. Data limited.
Carbon Dots / Graphene Quantum Dots / other Graphene Derivatives (Fluorescent Labelled)			
Bottom down methods from graphene / graphene oxide or bottom-up methods from various carbon sources followed by chemical functionalization.	Dependent on the utilized fluorophore. Excitation and Emission in Vis – NIR I	Highly fluorescent dyes can be applied.	Available studies suggest low toxicity. Data not concise at the present state.
Carbon Dots / Graphene Quantum Dots (Intrinsic Fluorescence)			
Bottom down methods from graphene / graphene oxide or bottom-up methods from various carbon sources followed by chemical functionalization.	Vis - Excitation wavelength dependent emission.	Super-resolution imaging possible. Fluorescence quantum yields vary largely dependent on the sample preparation.	Available studies suggest low toxicity. Data not concise at the present state.

Cite this: DOI: 10.1039/c0xx00000x

www.rsc.org/xxxxxx

ARTICLE TYPE

Notes and references

[a] *Istituto Italiano di Tecnologia (IIT), Nano Carbon Materials, Nanophysics Department, Via Morego 30, 16163 Genova, Italy. Tel: +39 – 010 – 71781 - 507; E-mail: silvia.giordani@iit.it*

[b] *School of Chemistry and Chemical Biology, Centre for Synthesis and Chemical Biology, University College Dublin, Dublin 4, Ireland.*

1 C. M. C. Tempany and B. J. McNeil, *JAMA,* 2001, **285**, 562-567.
2 H. Koo, M. S. Huh, J. H. Ryu, D.-E. Lee, I.-C. Sun, K. Choi, K. Kim and I. C. Kwon, *Nano Today,* 2011, **6**, 204-220.
3 S. K. Sahoo and V. Labhasetwar, *Drug Discov. Today,* 2003, **8**, 1112-1120.
4 S. M. Janib, A. S. Moses and J. A. MacKay, *Adv. Drug Deliv. Rev.,* 2010, **62**, 1052-1063.
5 N. C. Portney and M. Ozkan, *Anal. Bioanal. Chem.,* 2006, **384**, 620-630.
6 K. Kostarelos, A. Bianco and M. Prato, *Nature Nanotechnol.,* 2009, **4**, 627-633.
7 C. Fabbro, H. Ali-Boucetta, T. Da Ros, K. Kostarelos, A. Bianco and M. Prato, *Chem. Commun.,* 2012, **48**, 3911-3926.
8 E. H. L. Falcao and F. Wudl, *J. Chem. Technol. Biotechnol.,* 2007, **82**, 524-531.
9 J. L. Delgado, M. A. Herranz and N. Martin, *J. Mater. Chem.,* 2008, **18**, 1417-1426.
10 H. W. Kroto, J. R. Heath, S. C. O'Brien, R. F. Curl and R. E. Smalley, *Nature,* 1985, **318**, 162-163.
11 The schematic representation of the carbon nanohorn aggregate was prepared by Lengmartin. Copied and redistributed under CC BY-SA 3.0 (http://creativecommons.org/licenses/by-sa/3.0/) from http://upload.wikimedia.org/wikipedia/commons/4/4b/Carbon_Nanohorns_Aggregate.jpg; downloaded: 10/September/2014.
12 W. Bollmann and J. Spreadborough, *Nature,* 1960, **186**, 29-30.
13 S. Iijima, *Nature,* 1991, **354**, 56-58.
14 S. Iijima and T. Ichihashi, *Nature,* 1993, **363**, 603-605.
15 D. S. Bethune, C. H. Klang, M. S. de Vries, G. Gorman, R. Savoy and R. Beyers, *Nature,* 1993, **363**, 605-607.
16 H. Dai, *Acc. Chem. Res.,* 2002, **35**, 1035-1044.
17 A.-C. Depuis, *Prog. Mater. Sci.,* 2005, **50**, 929-961.
18 H. Hu, B. Zhao, M. E. Itkis and R. C. Haddon, *J. Phys. Chem. B,* 2003, **107**, 13838-13842.
19 K. Flavin, I. Kopf, E. Del Canto, C. Navio, C. Bittencourt and S. Giordani, *J. Mater. Chem.,* 2011, **21**, 17881-17887.
20 S. Iijima, M. Yudasaka, R. Yamada, S. Bandow, K. Suenaga, F. Kokai and K. Takahashi, *Chem. Phys. Lett.,* 1999, **309**, 165-170.
21 D. Kasuya, M. Yudasaka, K. Takahashi, F. Kokai and S. Iijima, *J. Phys. Chem. B,* 2002, **106**, 4947-4951.
22 V. V. Danilenko, *Phys. Solid State,* 2004, **46**, 595-599.
23 Y.-R. Chang, H.-Y. Lee, K. Chen, C.-C. Chang, D.-S. Tsai, C.-C. Fu, T.-S. Lim, Y.-K. Tzeng, C.-Y. Fang, C.-C. Han, H.-C. Chang and W. Fann, *Nature Nanotech.,* 2008, **3**, 284-288.
24 J.-P. Boudou, P. A. Curmi, F. Jelezko, J. Wrachtrup, P. Aubert, M. Sennour, G. Balasubramanian, R. Reuter, A. Thorel and E. Gaffet, *Nanotechnol.,* 2009, **20**, 235602.
25 D. Ugarte, *Nature,* 1992, **359**, 707-709.
26 L. Echegoyen, A. Ortiz, M. N. Chaur and A. J. Palkar, in *Chemistry of Nanocarbons,* ed. T. Akasaka, F. Wudl, and S. Nagase, John Wiley & Sons, Chichester, UK, 2010; pp. 463-483.
27 V. L. Kuznetsov, A. L. Chuvilin, Y. V. Butenko, I. Y. Mal'kov and V. M. Titov, *Chem. Phys. Lett.,* 1994, **222**, 343-348.
28 A. Palkar, F. Melin, C. M. Cardona, B. Elliott, A. K. Naskar, D. D. Edie, A. Kumbhar and L. Echegoyen, *Chem. Asian J.,* 2007, **2**, 625-633.
29 K. S. Novoselov, A. K. Geim, S. V. Morozov, D. Jiang, Y. Zhang, I. V. Grigorieva and A. A. Firsov, *Science,* 2004, **306**, 666-669.
30 A. K. Geim and K. S. Novoselov, *Nat. Materials,* 2007, **6**, 183-191.
31 M. J. Allen, V. C. Tung and R. B. Kaner, *Chem. Rev.,* 2010, **110**, 132-145.
32 C. N. R. Rao, U. Maitra and H. S. S. R. Matte, in *Graphene Synthesis, Properties, and Phenomena*, ed. C. N. R. Rao and A. K. Sood, Wiley-VCH Verlag GmbH & Co. KGaA, Weinheim, Germany, 2013, pp 1-47.
33 J. N. Coleman, *Acc. Chem. Res.,* 2013, **46**, 14-22.
34 K. R. Paton, E. Varrla, C. Backes, R. J. Smith, U. Khan, A. O'Neill, C. Boland, M. Lotya, O. M. Istrate, P. King, T. Higgins, S. Barwich, P. May, P. Puczkarski, I. Ahmed, M. Moebius, H. Pettersson, E. Long, J. Coelho, S. E. O'Brian, E. K. McGuire, B. M. Sanchez, G. S. Duesberg, N. McEvoy, T. J. Pennycook, C. Downing, A. Crossley, V. Nicolosi and J. N. Coleman, *Nature Mater.,* 2014, **13**, 624-630.
35 Y. Zhang, L. Zhang and C. Zhou, *Acc. Chem. Res.,* 2013 **46** 2329-2339.
36 V. Georgakilas, M. Otyepka, A. B. Bourlinos, V. Chandra, N. Kim, K. C. Kemp, P. Hobza, R. Zboril and K. S. Kim, *Chem. Rev.,* 2012, **112**, 6156-6214.
37 T. Kuila, S. Bose, A. K. Mishra, P. Khanra, N. H. Kim and J. H. Lee, *Prog. Mater. Sci.,* 2012, **57**, 1061-1105.
38 S. Eigler and A. Hirsch, *Angew. Chem. Int. Ed.,* 2014, **53**, 2-21.
39 J. Shen, Y. Zhu, X. Yang and C. Li, *Chem. Commun.,* 2012, **48**, 3686-3699.
40 Y. Song, S. Zhu and B. Yang, *RSC Adv.,* 2014, **4**, 27184-27200.
41 L. A. Ponomarenko, F. Schedin, M. I. Katsnelson, R. Yang, E. W. Hill, K. S. Novoselov and A. K. Geim, *Science*, 2008, **320**, 356-358.
42 L. Zhi and K. Müllen, *J. Mater. Chem.*, 2008, **18**, 1472-1484.
43 X. Yan, X. Cui, B. Li and L.-s. Li, *Nano Lett.*, 2010, **10**, 1869-1873.
44 R. Liu, D. Wu, X. Feng and K. Müllen, *J. Am. Chem. Soc.*, 2011, **133**, 15221-15223.
45 P. Singh, S. Campidelli, S. Giordani, D. Bonifazi, A. Bianco and M. Prato, *Chem. Soc. Rev.,* 2009, **38**, 2214-2230.
46 F. Hauke and A. Hirsch, in *Carbon Nanotubes and Related Structures: Synthesis, Characterization, Functionalization, and Applications*, ed. D. M. Guldi and N. Martin, Wiley-VCH Verlag GmbH & Co. KGaA, Weinheim, Germany, 2010, pp 135-198.
47 A. Krueger and D. Lang, *Adv. Funct. Mater.,* 2012, **22**, 890-906.
48 J. Bartelmess and S. Giordani, *Beilstein J. Nanotechnol.,* 2014, in press.
49 K. E. Sapsford, W. R. Algar, L. Berti, K. B. Gemmill, B. J. Casey, E. Oh, M. H. Stewart and I. L. Mednitz, *Chem. Rev.*, 2013, **113**, 1904-2074.
50 A. Nel, T. Xia, L. Mädler and N. Li, *Science,* 2006, **311**, 622-627.
51 K. Kostarelos *Nature Biotechnol.* 2008, **26**, 774-776.
52 D. Movia D. and S. Giordani, in *Handbook of Green Chemistry – Green Processes, Volume 8 – Green Nanoscience*, ed. A. Perosa and M. Selva, Wiley - VCH, Weinheim, Germany, 2012; pp. 175-216.
53 C. A. Poland, R. Duffin, I. Kinloch, A. Maynard, W. A. H. Wallace, A. Seaton, V. Stone, S. Brown, W. MacNee and K. Donaldson, *Nature Nanotechnol.,* 2008, **3**, 423-428.
54 K. Donaldson, R. Aitken, L. Tran, V. Stone, R. Duffin, G. Forrest and A. Alexander, *Toxicol. Sci.,* 2006, **92**, 5-22.
55 C.-w. Lam, J. T. James, R. McCluskey, S. Arepalli and R. L. Hunter, *Crit. Rev. Tox.,* 2006, **36**, 189-217.

[56] S. K. Smart, A. I. Cassady, G. Q. Lu and D. J. Martin, *Carbon,* 2006, **44**, 1034-1047.
[57] D. Movia, A. P. Mello, D. Bazou, Y. Volkov and S. Giordani, *ACS Nano*, 2011, **5**, 9278-9290.
[58] N. Saito, H. Haniu, Y. Usui, K. Aoki, K. Hara, S. Takanashi, M. Shimizu, N. Narita, M. Okamoto, S. Kobayashi, H. Nomura, H. Kato, N. Nishimura, S. Taruta and M. Endo, *Chem. Rev.,* 2014, **114**, 6040-6079.
[59] H.-F. Cui, S. K. Vashist, K. Al-Rubeaan, J. H. T. Luong and F.-S. Sheu, *Chem. Res. Toxicol.,* 2010, **23**, 1131-1147.
[60] H. Ali-Boucetta, A. Nunes, R. Sainz, M. A. Herrero, B. Tian, M. Prato, A. Bianco and K. Kostarelos, *Angew. Chem. Int. Ed.,* 2013, **52**, 2274-2278.
[61] J. Miyawaki, M. Yudasaka, T. Azami, Y. Kubo and S. Iijima, *ACS Nano,* 2008, **2**, 213-226.
[62] V. C. Sanchez, A. Jachak, R. H. Hurt and A. B. Kane, *Chem. Res. Toxicol.,* 2012, **25**, 15-34.
[63] A. B. Seabra, A. J. Paula, R. de Lima, O. L. Alves and N. Duran, *Chem. Res. Toxicol.,* 2014, **27**, 159-168.
[64] A. M. Schrand, H. Huang, C. Carlson, J. J. Schlager, E. Osawa, S. M. Hussain and L. Dai, *J. Phys. Chem. B,* 2007 **111**, 2-7.
[65] Y. Xing and L. Dai, *Nanomedicine,* 2009, **4**, 207-218.
[66] Y. Zhu, J. Li, Y. Zhang, X. Yang, N. Chen, Y. Sun, Y. Zhao, C. Fan and Q. Huang, *Theranostics,* 2012, **2**, 302-312.
[67] L. Ding, J. Stilwell, T. Zhang, O. Elboudwarej, H. Jiang, J. P. Selegue, P. A. Cooke, J. W. Gray and F. F. Chen, *Nano Lett.,* 2005, **5**, 2448-2464.
[68] J. Luszczyn, M. E. Plonska-Brzezinska, A. Palkar, A. T. Dubis, A. Simionescu, D. T. Simionescu, B. Kalska-Szostko, K. Winkler and L. Echegoyen, *Chem. Eur. J.,* 2010, **16**, 4870-4880.
[69] M. Yang, K. Flavin, G. Radics, C. H. A. Hearnden, G. J. McManus, B. Moran, A. Villalta-Cerdas, L. A. Echegoyen, S. Giordani and E. C. Lavelle, *Small*, 2013, **9**, 4194-4206.
[70] R. Weissleder, *Nature Biotechnol.,* 2001, **19**, 316-317.
[71] A. M. Smith, M. C. Mancini and S. Nie, *Nature Nanotechol.,* 2009, **4**, 710-711.
[72] Y. T. Lim, S. Kim, A. Nakayama, N. E. Stott, M. G. Bawendi and J. V. Frangioni, *Mol. Imaging,* 2003, **2**, 50-64.
[73] M. J. O'Connell, S. M. Bachilo, C. B. Huffman, V. C. Moore, M. S. Strano, E. H. Haroz, K. L. Rialon, P. J. Boul, W. H. Noon, C. Kittrell, J. Ma, R. H. Hauge, R. B. Weisman and R. E. Smalley, *Science,* 2002, **297**, 593-596.
[74] P. Cherukuri, S. M. Bachilo, S. H. Litovsky and R. B. Weisman, *J. Am. Chem. Soc.,* 2004, **126**, 15638-15639.
[75] D. A. Heller, S. Baik, T. E. Eurell and M. S. Strano, *Adv. Mater.,* 2005, **17**, 2793-2799.
[76] S. Giordani, S. D. Bergin, V. Nicolosi, S. Lebedkin, M. M. Kappes, W. J. Blau and J. N. Coleman, *J. Phys. Chem. B,* 2006, **110**, 15708-15718.
[77] P. Avouris, M. Freitag and V. Perebeinos, *Nature Photon.,* 2008, **2**, 341-350.
[78] D. Movia, E. Del Canto and S. Giordani, *J. Phys. Chem. C,* 2010, **114**, 18407-18413.
[79] K. Welsher, S. P. Sherlock and H. Dai, *Proc. Natl. Acad. Sci.,* 2011, **108**, 8943-8948.
[80] S. M. Bachilo, M. S. Strano, C. Kittrell, R. H. Hauge, R. E. Smalley and R. B. Weisman, *Science,* 2002, **298**, 2361-2366.
[81] L. J. Carlson, S. E. Maccagnano, M. Zheng, J. Silcox and T. D. Krauss, *Nano Lett.,* 2007, **7**, 3698-3703.
[82] J. Crochet, M. Clemens, and T. Hertel, *J. Am. Chem. Soc.*, 2007, **129**, 8058-8059.
[83] J. Lefebvre, D. G. Austing, J. Bond and P. Finnie, *Nano Lett*., 2006, **6**, 1603-1608.
[84] S. Ghosh, S. M. Bachilo, R. A. Simonette, K. M. Beckingham and R. B. Weisman, *Science*, 2010, **330**, 1656-1659.
[85] Y. Piao, B. Meany, L. R. Powell, N. Valley, H. Kwon, G. C. Schatz and Y. Wang, *Nature Chem.*, 2013, **5**, 840-845.
[86] J. E. Riggs, Z. Guo, D. L. Carroll and Y.-P. Sun, *J. Am. Chem. Soc.,* 2000, **122**, 5879-5880.
[87] Y. Lin, B. Zhou, R. B. Martin, K. B. Henbest, B. A. Harruff, J. E. Riggs, Z.-X. Guo, L. F. Allard and Y.-P. Sun, *J. Phys. Chem. B,* 2005, **109**, 14779-14782.
[88] L. Lacerda, G. Pastorin, W. Wu, M. Prato, A. Bianco and K. Kostarelos, *Adv. Funct. Mater.,* 2006, **16**, 1839-1846.
[89] T. Gokus, R. R. Nair, A. Bonetti, M. Böhmler, A. Lombardo, K. S. Novoselov, A. K. Geim, A. C. Ferrari and A. Hartschuh, *ACS Nano*, 2009, **3**, 3963-3968.
[90] X. Wang, L. Cao, S.-T. Yang, F. Lu, M. J. Meziani, L. Tian, K. W. Sun, M. A. Bloodgood and Y.-P. Sun, *Angew. Chem. Int. Ed.,* 2010, **49**, 5310-5314.
[91] S. Srivastava and N. S. Gajbhiye, *ChemPhysChem,* 2011, **12**, 2624-2632.
[92] M. O. Dekaliuk, O. Viagin, Y. V. Malyukin and A. P. Demchenko, *Phys. Chem. Chem. Phys.,* 2014, **16**, 16075-16084.
[93] L. Cao, M. J. Meziani, S. Sahu and Y.-P. Sun, *Acc. Chem. Res.,* 2013, **46**, 171-180.
[94] Y.-P. Sun, B. Zhou, Y. Lin, W. Wang, K. A. S. Fernando, P. Pathak, M. J. Meziani, B. A. Harruff, X. Wang, H. Wang, P. G. Luo, H. Yang, M. E. Kose, B. Chen, L. M. Veca and S.-Y. Xie, *J. Am. Chem. Soc.,* 2006, **128**, 7756-7757.
[95] S. C. Cushing, M. Li, F. Huang and N. Wu, *ACS Nano,* 2014, **8**, 1002-1013.
[96] V. N. Mochalin, O. Shenderova, D. Ho and Y. Gogotsi, *Nature Nanotech.,* 2012, **7**, 11-23.
[97] J. Havlik, V. Petrakova, I. Rehor, V. Petrak, M. Gulka, J. Stursa, J. Kucka, J. Ralis, T. Rendler, S.-Y. Lee, R. Reuter, J. Wrachtrup, M. Ledvina, M. Nesladek and P. Cigler, *Nanoscale,* 2013, **5**, 3208-3211.
[98] V. Georgakilas, D. M. Guldi, R. Signorini, R. Bozio and M. Prato, *J. Am. Chem. Soc.,* 2003, **125**, 14268-14269.
[99] C. T. Cioffi, A. Palkar, F. Melin, A. Kumbhar, L. Echegoyen, M. Melle-Franco, F. Zerbetto, G. M. A. Rahman, C. Ehli, V. Sgobba, D. M. Guldi and M. Prato, *Chem. Eur. J.,* 2009, **15**, 4419-4427.
[100] M. Ghosh, S. K. Sonkar, M. Saxena and S. Sarkar, *Small,* 2011, **7**, 3170-3177.
[101] P. Allongue, M. Delamar, B. Desbat, O. Fagebaume, R. Hitmi, J. Pinson, and J.-M. Savéant, *J. Am. Chem. Soc.,* 1997, **119**, 201-207.
[102] J. L. Bahr, J. Yang, D. V. Kosynkin, M. J. Bronikowski, R. E. Smalley and J. M. Tour, *J. Am. Chem. Soc.,* 2001, **123**, 6536-6542.
[103] J. L. Bahr and J. M. Tour, *Chem. Mater.,* 2001, **13**, 3823-3824.
[104] K. Flavin, M. N. Chaur, L. Echegoyen and S. Giordani, *Org. Lett.,* 2010, **12**, 840-843.
[105] Y. Liang, M. Ozawa and A. Krueger, *ACS Nano,* 2009, **3**, 2288-2296.
[106] T. Meinhardt, D. Lang, H. Dill and A. Krueger, *Adv. Funct. Mater.,* 2011, **21**, 494-500.
[107] M.-E. Ragoussi, S. Casado, R. Ribeiro-Viana, G. de la Torre, J. Rojo and T. Torres, *Chem. Sci.,* 2013, **4**, 4035-4041.
[108] M.-E. Ragoussi, G. Katsukis, A. Roth, J. Malig, G. de la Torre, D. M. Guldi and T. Torres, *J. Am. Chem. Soc.,* 2014, **136**, 4593-4598.
[109] L. Cognet, D. A. Tsyboulski, J.-D. R. Rocha, C. D. Doyle, J. M. Tour and R. B. Weisman, *Science*, 2007, **316**, 1465-1468.
[110] Y.-L. Zhao and J. F. Stoddart, *Acc. Chem. Res.,* 2009, **42**, 1161-1171.
[111] M. A. Herranz and N. Martin, in *Carbon Nanotubes and Related Structures: Synthesis, Characterization, Functionalization, and Applications*, ed. D. M. Guldi and N. Martin, Wiley-VCH Verlag GmbH & Co. KGaA, Weinheim, Germany, 2010, pp 103-134.
[112] D. M. Guldi, G. M. A. Rahman, N. Jux, N. Tagmatarchis and M. Prato, *Angew. Chem. Int. Ed.,* 2004, **116**, 5642-5646.
[113] E. Maligaspe, A. S. D. Sandanayaka, T. Hasobe, O. Ito and F. D'Souza, *J. Am. Chem. Soc.,* 2010, **132**, 8158-8164.
[114] J. Bartelmess, B. Ballesteros, G. de la Torre, D. Kiessling, S. Campidelli, M. Prato, T. Torres and D. M. Guldi, *J. Am. Chem. Soc.,* 2010, **132**, 16202-16211.
[115] J. Bartelmess, C. Ehli, J.-J. Cid, M. Garcia-Iglesias, P. Vazquez, T. Torres and D. M. Guldi, *Chem. Sci.,* 2011, **2**, 652-660.

[116] J. Malig, N. Jux, D. Kiessling, J.-J. Cid, P. Vazquez, T. Torres and D. M. Guldi, *Angew. Chem. Int. Ed.,* 2011, **50**, 3561-3565.
[117] T. Kwon, G. Lee, H. Choi, M. S. Strano and W.-J. Kim, *Nanoscale,* 2013, **5**, 6773-6778.
[118] N. Nakayama-Ratchford, S. Bangsaruntip, X. Sun, K. Welsher and H. Dai, *J. Am. Chem. Soc.,* 2007, **129**, 2448-2449.
[119] M. Zheng, A. Jagota, M. S. Strano, A. P. Santos, P. Barone, S. G. Chou, B. A. Diner, M. S. Dresselhaus, R. S. McLean, G. B. Onoa, G. G. Samsonidze, E. D. Semke, M. Usrey and D. J. Walls, *Science,* 2003, **302**, 1545-1548.
[120] Q. Lu, J. M. Moore, G. Huang, A. S. Mount, A. M. Rao, L. L. Larcom and P. C. Ke, *Nano Lett.,* 2004, **4**, 2473-2477.
[121] N. W. S. Kam, M. O'Connell, J. A. Wisdom and H. Dai, *Proc. Natl. Acad. Sci.,* 2005, **102**, 11600-11605.
[122] H. Cathcart, S. Quinn, V. Nicolosi, J. M. Kelly, W. J. Blau and J. N. Coleman, *J. Phys. Chem. C,* 2007, **111**, 66-74.
[123] H. Cathcart, V. Nicolosi, J. M. Hughes, W. J. Blau, J. M. Kelly, S. J. Quinn and J. N. Coleman, *J. Am. Chem. Soc.,* 2008, **130**, 12734-12744.
[124] N. W. S. Kam and H. Dai, *J. Am. Chem. Soc.,* 2005, **127**, 6021-6026.
[125] G. Bottari, G. de la Torre, D. M. Guldi and T. Torres, *Chem. Rev.,* 2010, **110**, 6768-6816.
[126] D. Baskaran, J. W. Mays, X. P. Zhang and M. S. Bratcher, *J. Am. Chem. Soc.,* 2005, **127**, 6916-6917.
[127] T. Hasobe, S. Fukuzumi and P. V. Kamat, *J. Am. Chem. Soc.,* 2005, **127**, 11884.
[128] G. M. A. Rahman, D. M. Guldi, S. Campidelli and M. Prato, *J. Mater. Chem.,* 2006, **16**, 62-65.
[129] K. Flavin, K. Lawrence, J. Bartelmess, M. Tasior, C. Navio, C. Bittencourt, D. F. O.'Shea and S. Giordani, *ACS Nano,* 2011, **5**, 1198-1206.
[130] M. S. Dresselhaus, G. Dresselhaus and M. Hofmann, *Vib. Spec.,* 2007, **45**, 71-81.
[131] M. S. Dresselhaus, A. Jorio, M. Hofmann, G. Dresselhaus and R. Saito, *Nano Lett.,* 2010, **10**, 751-758.
[132] D. Roy, M. Chhowalla, H. Wang, N. Sano, I. Alexandrou, T. W. Clyne and G. A. J. Amaratunga, *Chem. Phys. Lett.,* 2003, **373**, 52-56.
[133] Q. Tu and C. Chang, *Nanomedicine: NBM,* 2012, **8**, 545-558.
[134] M. Vendrell, K. K. Maiti, K. Dhaliwal and Y.-T. Chang, *Trends Biotechnol.,* 2013, **31**, 249-257.
[135] P. T. Araujo, P. B. C. Pesce, M. S. Dresselhaus, K. Sato, R. Saito and A. Jorio, *Physica E,* 2010, **42**, 1251-1261.
[136] P. C. Eklund, J. M. Holden and R. A Jishi, *Carbon,* 1995, **33**, 959-972.
[137] Z. Chen, S. M. Tabakman, A. P. Goodwin, M. K. Kattah, D. Daranciang, X. Wang, G. Zhang, X. Li, P. J. Utz, K. Jiang, S. Fan and H. Dai, *Nature Biotechnol.,* 2008, **26**, 1285-1292.
[138] Z. Liu, X. Li, S. C. Tabakman, K. Jiang, S. Fan and H. Dai, *J. Am. Chem. Soc.,* 2008, **130**, 13540-13541.
[139] Z. Liu, S. Tabakman, S. Sherlock, X. Li, Z. Chen, K. Jiang, S. Fan and H. Dai, *Nano Res.,* 2010, **3**, 222-233.
[140] E. Gaufrès, N. Y.-W. Tang, F. Lapointe, J. Cabana, M.-A. Nadon, N. Cottonye, F. Raymond, T. Skopek and R. Martel, *Nature Photonics*, 2014, **8**, 72-78.
[141] B. S. Harrison and A. Atala, *Biomaterials,* 2007, **28**, 344-353.
[142] H. Hong, T. Gao and W. Cai, *Nano Today,* 2009, **4**, 252-261.
[143] Z. Liu, K. Yang and S.-T. Lee, *J. Mater. Chem.,* 2011, **21**, 586-598.
[144] H. Gong, R. Peng and Z. Liu, *Adv. Drug Deliv. Rev.,* 2013, **65**, 1951-1963.
[145] L. Nie and X. Chen, *Chem. Soc. Rev.,* 2014, **43**, 7132-7170..
[146] B. S. Wong, S. L. Yoong, A. Jagusiak, T. Panczyk, H. K. Ho, W. H. Ang and G. Pastorin, *Adv. Drug. Deliv. Rev.,* 2013, **66**, 1964-2015.
[147] D. Pantarotto, J.-P. Briand, M. Prato and A. Bianco, *Chem. Commun.,* 2004, 16-17.
[148] N. W. S. Kam, T. C. Jessop, P. A. Wender and H. Dai, *J. Am. Chem. Soc.,* 2004, **126**, 6850-6851.
[149] W. Wu, S. Wieckowski, G. Pastorin, M. Benincasa, C. Klumpp, J.-P. Briand, R. Gennaro, M. Prato and A. Bianco, *Angew. Chem. Int. Ed.,* 2005, **44**, 6358-6362.
[150] K. Kostarelos, L. Lacerda, G. Pastorin, W. Wu, S. Wieckowski, J. Luangsivilay, S. Godefroy, D. Pantarotto, J.-P. Briand, S. Muller, M. Prato and A. Bianco, *Nature Nanotechnol.,* 2007, **2**, 108-113.
[151] R. P. Feazell, N. Nakayama-Ratchford, H. Dai and S. J. Lippard, *J. Am. Chem. Soc.,* 2007, **129**, 8438-8439.
[152] S. Dhar, Z. Liu, J. Thomale, H. Dai and S. J. Lippard, *J. Am. Chem. Soc.,* 2008, **130**, 11467-11476.
[153] G. Pastorin, W. Wu, S. Wieckowski, J.-P. Briand, K. Kostarelos, M. Prato and A. Bianco, *Chem. Commun.,* 2006, 1182-1184.
[154] J. Chen, S. Chen, X. Zhao, L. V. Kuznetsova, S. S. Wong and I. Ojima, *J. Am. Chem. Soc.,* 2008, **130**, 16778-16785.
[155] E. Heister, V. Neves, C. Tilmaciu, K. Lipert, V. S. Beltran, H. M. Coley, S. R. P. Silva and J. McFadden, *Carbon,* 2009, **47**, 2152-2160.
[156] N. W. S. Kam, Z. Liu and H. Dai, *Angew. Chem. Int. Ed.,* 2006, **45**, 577-581.
[157] Z. Liu, X. Sun N. Nakayama-Ratchford and H. Dai, *ACS Nano,* 2007, **1**, 50-56.
[158] X. Zhang, L. Meng, Q. Lu, Z. Fei and P. J. Dyson, *Biomaterials,* 2009, **30**, 6041-6047.
[159] N. W. S. Kam, Z. Liu and H. Dai, *J. Am. Chem. Soc.,* 2005, **127**, 12492-12493.
[160] H. K. Moon, C. I. Chang, D.-K. Lee and H. C. Choi, *Nano Res.,* 2008, **1**, 351-360.
[161] L. Beqa, Z. Fan, A. K. Singh, D. Senapati and P. C. Ray, *ACS Appl. Mater. Interfaces,* 2011, **3**, 3316-3324.
[162] X. Michalet, F. F. Pinaud, L. A. Bentolila, J. M. Tsay, S. Doose, J. J. Li, G. Sundaresan, A. M. Wu, S. S. Gambhir and S. Weiss, *Science,* 2005, **307**, 538-544.
[163] V. Biju, T. Itoh and M. Ishikawa, *Chem. Soc. Rev.,* 2010, **39**, 3031-3056.
[164] E. Petryayeva, W. R. Algar and I. L. Medintz, *Appl. Spectrosc.,* 2013, **67**, 215-252.
[165] M. Bottini, F. Cerignoli, M. I. Dawson, A. Magrini, N. Rosato and T. Mustelin, *Biomacromolecules,* 2006, **7**, 2259-2263.
[166] D. Shi, Y. Guo, Z. Dong, J. Lian, W. Wang, G. Liu, L. Wang and R. C. Ewing, *Adv. Mater.,* 2007, **19**, 4033-4037.
[167] Y. Zhang, W. Qin, H. Tang, F. Yan, L. Tan, Q. Xie, M. Ma, Y. Zhang and S. Yao, *Colloids Surf., B,* 2011, **87**, 346-352.
[168] H. Wang, Z. Wang, M. Ye, S. Zong, M. Li, P. Chen, X. Ma and Y. Cui, *Talanta,* 2014, **119**, 144-150.
[169] A. A. Bhirde, V. Patel, J. Gavard, G. Zhang, A. A. Sousa, A. Masedunskas, R. D. Leapman, R. Weigert, J. S. Gutkind and J. F. Rusling, *ACS Nano,* 2009, **3**, 307-316.
[170] M.-L. Chen, Y.-J. He, X.-W. Chen and J.-H. Wang, *Langmuir,* 2012, **28**, 16469-16476.
[171] L. V. Nair, Y. Nagaoka, T. Maekawa, D. Sakthikumar and R. S. Jayasree, *Small,* 2014, **10**, 2771-2775.
[172] I. P. Chang, K. C. Hwang and C.-S. Chiang, *J. Am. Chem. Soc.,* 2008, **130**, 15476-15482.
[173] S. Vial, C. Mansuy, S. Sagan, T. Irinopoulou, F. Burlina, J.-P. Boudou, G. Chassaing and S. Lavielle, *ChemBioChem,* 2008, **9**, 2113-2119.
[174] X.-Q. Zhang, R. Lam, X. Xu, E. K. Chow, H.-J. Kim and D. Ho, *Adv. Mater.,* 2011, **23**, 4770-4775.
[175] E. K. Chow, X.-Q. Zhang, M. Chen, R. Lam, E. Robinson, H. Huang, D. Schaffer, E. Osawa, A. Goga and D. Ho, *Science Transl. Med.,* 2011, **3**, 73ra21.
[176] A. D. Salaam, P. Hwang, R. McIntosh, H. N. Green, H.-W. Jun and D. Dean, *Beilstein J. Nanotechnol.,* 2014, **5**, 937-945.
[177] J. Bartelmess, E. De Luca, A. Signorelli, M. Baldrighi, M. Becce, R. Brescia, V. Nardone, E. Parisini, P. P. Pompa, E. Echegoyen and S. Giordani, *Nanoscale,* 2014, **6**, 13761-13769.
[178] S. Giordani, J. Bartelmess, M. Frasconi, I. Biondi, S. Cheung, M. Grossi, D. Wu, L. Echegoyen and D. F. O'Shea, *J. Mater. Chem. B,* 2014, **2**, 7459-7463.

[179] J. Murtagh, D. O. Frimannsson and D. F. O'Shea *Org. Lett.* 2009, **11**, 5386-5389.
[180] C. Peng, W. Hu, Y. Zhou, C. Fan and Q. Huang, *Small,* 2010, **6**, 1686-1692.
[181] M.-L. Chen, J.-W. Liu, B. Hu, M.-L. Chen and J.-H. Wang, *Analyst,* 2011, **136**, 4277-4283.
[182] T. N. Narayanan, B. K. Gupka, S. A. Vithayathil, R. R. Aburto, S. A. Mani, J. Taha-Tijerina, B. Xie, B. A. Kaipparettu, S. V. Torti and P. M. Ajayan, *Adv. Mater.,* 2012, **24**, 2992-2998.
[183] S. Sreejith, X. Ma and Y. Zhao, *J. Am. Chem. Soc.,* 2012, **134**, 17346-17349.
[184] G. Xie, J. Cheng, Y. Li, P. Xi, F. Chen, H. Liu, F. Hou, Y. Shi, L. Huang, Z. Xu, D. Bai and Z. Zeng, *J. Mater. Chem.,* 2012, **22**, 9308-9314.
[185] C. Guo, B. Book-Newell and J. Irudayaraj, *Chem. Commun.,* 2011, **47**, 12658-12660.
[186] K. Yang, S. Zhang, G. Zhang, X. Sun, S.-T. Lee and Z. Liu, *Nano Lett*., 2010, **10**, 3318-3323.
[187] G. Gollavelli and Y.-C. Ling, *Biomaterials,* 2012, **33**, 2532-2545.
[188] L. Zhou, W. Wang, J. Tang, J.-H. Zhou, H.-J. Jiang and J. Shen, *Chem. Eur. J.,* 2011, **17**, 12084-12091.
[189] L. Zhou, L. Zhou, S. Wei, X. Ge, J. Zhou, H. Jiang, F. Li and J. Shen, *J. Photochem. Photobiol., B,* 2014, **135**, 7-16.
[190] P. Huang, C. Xu, J. Lin, C. Wang, X. Wang, C. Zhang, X. Zhou, S. Guo and D. Cui, *Theranostics,* 2011, **1**, 240-250.
[191] B. Tian, C. Wang, S. Zhang, L. Feng and Z. Liu, *ACS Nano,* 2011, **5**, 7000-7009.
[192] P. Rong, K. Yang, A. Srivastan, D. O. Kiesewetter, X. Yue, F. Wang, L. Nie, A. Bhirde, Z. Wang, Z. Liu, G. Niu, W. Wang and X. Chen, *Theranostics,* 2014, **4**, 229-239.
[193] C. Wang, J. Li, C. Amatore, Y. Chen, H. Jiang and X.-M.Wang, *Angew. Chem. Int. Ed.,* 2011, **50**, 11644-11648.
[194] K. Liu, J.-J. Zhang, F.-F. Cheng, T.-T. Zheng, C. Wang and J.-J. Zhu, *J. Mater. Chem.,* 2011, **21**, 12034-12040.
[195] A. R. Maity, A. Chakraborty, A. Mondal and N. R. Jana, *Nanoscale,* 2014, **6**, 2752-2758.
[196] T. Mosaiab, I. In and S. Y. Park, *Macromol. Rapid Commun.,* 2013, **34**, 1408-1415.
[197] S. M. Sharker, C. J. Jeong, S. M. Kim, J.-E. Lee, J. H. Jeong, I. In, H. Lee and S. Y. Park *Chem. Asian J.* 2014, **9**, 2921-2927.
[198] J. T. Robinson, S. M. Tabakman, Y. Liang, H. Wang, H. S. Casalongue, D. Vinh and H. Dai, *J. Am. Chem. Soc.,* 2011, **133**, 6825-6831.
[199] M. Zhang, T. Murakami, K. Ajima, K. Tsuchida, A. S. D. Sandanayaka, O. Ito, S. iijima and M. Yudasaka, *Proc. Natl. Acad. Sci.,* 2008, **105**, 14773-14778.
[200] J. Zhang, J. Ge, M. D. Shultz, E. Chung, G. Singh, C. Shu, P. P. Fatouros, S. C. Henderson, F. D. Corwin, D. B. Geohegan, A. A. Puretzky, C. M. Rouleau, K. More, C. Rylander, M. N. Rylander, H. W. Gibson and H. C. Dorn, *Nano Lett.,* 2010, **10**, 2843-2848.
[201] J. Li, Y. He, Z. He, P. Zeng and S. Xu, *Anal. Biochem.,* 2012, **428**, 4-6.
[202] K. A. Zimmermann, D. L. Inglefield Jr., J. Zhang, H. C. Dorn, T. E. Long, C. G. Rylander and M. N. Rylander, *J. Nanopart. Res.,* 2014, **16**:2078.
[203] J. Li, Z. He, C. Guo, L. Wang and S. Xu, *J. Lumin.,* 2014, **145**, 78-80.
[204] L. Lacerda, G. Pastorin, D. Gathercole, J. Buddle, M. Prato, A. Bianco and K. Kostarelos, *Adv. Mater.,* 2007, **19**, 1480-1484.
[205] K. Welsher, Z. Liu, D. Daranciang and H. Dai, *Nano Lett.,* 2008, **8**, 586-590.
[206] H. Jin, D. A. Heller and M. S. Strano, *Nano Lett.,* 2008, **8**, 1577-1585.
[207] H. Jin,, D. A. Heller, R. Sharma and M. S. Strano, *ACS Nano,* 2009, **3**, 149-158.
[208] P. Cherukuri, C. J. Gannon, T. K. Leeuw, H. K. Schmidt, R. E. Smalley, S. A. Curley and R. B. Weisman, *Proc. Natl. Acad. Sci.,* 2006, **103**, 18882-18886.
[209] T. K. Leeuw, R. M. Reith, R. A. Simonette, M. E. Harden, P. Cherukuri, D. A. Tsyboulski, K. M. Beckingham and R. B. Weisman, *Nano Lett.,* 2007, **7**, 2650-2654.
[210] K. Welsher, Z. Liu, S. P. Sherlock, J. T. Robinson, Z. Chen, D. Daranciang and H. Dai, *Nature Nanotechnol.,* 2009, **4**, 773-780.
[211] J. T. Robinson, K. Welsher, S. M. Tabakman, S. P. Sherlock, H. Wang, R. Luong and H. Dai, *Nano Res.,* 2010, **3**, 779-793.
[212] J. T. Robinson, G. Hong, Y. Liang, B. Zhang, O. K. Yaghi and H. Dai, *J. Am. Chem. Soc.,* 2012, **134**, 10664-10669.
[213] S. Diao, G. Hong, J. T. Ribinson, L. Jiao, A. L. Antaris, J. Z. Wu, C. L. Choi and H. Dai, *J. Am. Chem. Soc.,* 2012, **134**, 16971-16974.
[214] A. L. Antaris, J. T. Robinson, O. K. Yaghi, G. Hong, S. Diao, R. Luong and H. Dai, *ACS Nano,* 2013, **7**, 3644-3652.
[215] G. Hong, J. C. Lee, J. T. Robinson, U. Raaz, L. Xie, N. F. Huang, J. P. Cooke and H. Dai, *Nature Med.,* 2012, **18**, 1841-1846.
[216] H. Yi, D. Ghosh, M.-H. Ham, J. Qi, P. W. Barone, M. S. Strano and A. M. Belcher, *Nano Lett.,* 2012, **12**, 1176-1183.
[217] J. H. Bisesi, Jr., J. Merten, K. Liu, A. N. Parks, A. R. M. Afrooz, J. B. Glenn, S. J. Klaine, A. S. Kane, N. B. Saleh, P. L. Ferguson and T. Sabo-Attwood, *Environ. Sci. Technol.,* 2014, **48**, 1973-1983.
[218] J. Shen, Y. Zhu, X. Yang and C Li, *Chem. Commun.,* 2012, **48**, 3686-3699.
[219] S. Zhu, J. Zhang, C. Qiao, S. Tang, Y. Li, W. Yuan, B. Li, L. Tian, F. Liu, R. Hu, H. Gao, H. Wei, H. Zhang, H. Sun and B. Yang, *Chem. Commun.,* 2011, **47**, 6858-6860.
[220] D. Pan, L. Guo, J. Zhang, C. Xi, Q. Xue, H. Huang, J. Li, Z. Zhang, W. Yu, Z. Chen, Z. Li and M. Wu, *J. Mater. Chem.,* 2012, **22**, 3314-3318.
[221] Y. Dong, C. Chen, X. Zheng, L. Gao, Z. Cui, H. Yang, C. Guo, Y. Chi and C. M. Li, *J. Mater. Chem.,* 2012, **22**, 8764-8766.
[222] J. Peng, W. Gao, B. K. Gupta, Z. Liu, R. Romero-Aburto, L. Ge, L. Song, L. B. Alemany, X. Zhan, G. Gao, S. A. Vithayathil, B. A. Kaiparettu, A. A. Marti, T. Hayashi, J.-J. Zhu and P. M. Ajayan, *Nano Lett.,* 2012, **12**, 844-849.
[223] S. Zhu, Q. Meng, L. Wang, J. Zhang, Y. Song, H. Jin, K. Zhang, H. Sun, H. Wang and B. Yang, *Angew. Chem. Int. Ed.,* 2013, **52**, 3953-3957.
[224] M. Zhang, L. Bai, W. Shang, W. Xie, H. Ma, Y. Fu, D. Fang, H. Sun, L. Fan, M. Han, C. Liu and S. Yang, *J. Mater. Chem.,* 2012, **22**, 7461-7469.
[225] X. Zhang, S. Wang, M. Liu, B. Yang, L. Feng, Y. Ji, L. Tao and Y. Wei, *Phys. Chem. Chem. Phys.,* 2013, **15**, 19013-19018.
[226] H. Sun, L. Wu, N. Gao, J. Ren and X. Qu, *Appl. Mater. Interfaces,* 2013, **5**, 1174-1179.
[227] M. Algarra, M. Pérez-Martin, M. Cifuentes-Rueda, J. Jiménez-Jiménez, J. C. G. Esteves DaSilva, T. J. Bandosz, E. Rodriguez-Castellon, J. T. L. Navarrete and J. Casado, *Nanoscale*, 2014, **6**, 9071-9077.
[228] C. Shen, Y. Sun, J. Wang and Y. Lu, *Nanoscale,* 2014, **6**, 9139-9147.
[229] J. Wei, X. Zhang, Y. Sheng, J. Shen, P. Huang, S. Guo, J. Pan, B. Liu and B. Feng, *New J. Chem.,* 2014, **38**, 906-909.
[230] J. Gong, X. An and X. Yan, *New J. Chem.,* 2014, **38**, 1376-1379.
[231] X. Liu, N. Xiao, N. Gong, H. Wang, X. Shi, W. Gu and L. Ye, *Carbon,* 2014, **68**, 258-264.
[232] G. Leménager, E. De Luca, Y.-S. Sun and P. P. Pompa, *Nanoscale,* 2014, **6**, 8617-8623.
[233] X. Gong, Q. Hu, M. C. Paau, Y. Zhang, S. Shuang, C. Dong and M. M. F. Choi, *Nanoscale,* 2014, **6**, 8162-8170.
[234] Z. Fan, Y. Li, X. Li, L. Fan, S. Zhou, D. Fang and S. Yang, *Carbon,* 2014, **70**, 149-156.
[235] L. Cao, X. Wang, M. J. Meziani, F. Lu, H. Wang, P. G. Luo, Y. Lin, B. A. Harruff, L. M. Veca, D. Murray, S.-Y. Xie and Y.-P. Sun, *J. Am. Chem. Soc.,* 2007, **129**, 11318-11319.
[236] J.-J. Li, H.-C. Bao, X.-L. Hou, L. Sun, X.-G. Wang and M. Gu, *Angew. Chem. Int. Ed.,* 2012, **51**, 1830-1834.
[237] S. Zhu, J. Zhang, S. Tang, C. Qiao, L. Wang, H. Wang, X. Liu, B. Li, Y. Li, W. Yu, X. Wang, H. Sun and B. Yang, *Adv. Funct. Mater.,* 2012, **22**, 4732-4740.

[238] B. Kong, A. Zhu, C. Ding, X. Zhao, B. Li and Y. Tian, *Adv. Mater.,* 2012, **24**, 5844-5848.

[239] L. Cao, S.-T. Yang, X. Wang, P. G. Luo, J.-H. Liu, S. Sahu, Y. Liu and Y.-P. Sun, *Theranostics,* 2012, **2**, 295-301.

[240] S. Ruan, J. Qian, S. Shen, J. Zhu, X. Jiang, Q. He and H Gao, *Nanoscale,* 2014, **6**, 10040-10047.

[241] J. Qian, D. Wang, F.-H. Cai, W. Xi, L. Peng, Z.-F. Zhu, H. He, M.-L. Hu and S. He, *Angew. Chem. Int. Ed.,* 2012, **51**, 10570-10575.

[242] Y. Y. Hui, C.-L. Cheng and H.-C. Chang, *J. Phys. D: Appl. Phys.,* 2010, **43**, 374021.

[243] C.-C. Fu, H.-Y. Lee, K. Chen, T.-S. Lim, H.-Y. Wu, P.-K. Lin, P.-K. Wei, P.-H. Tsao, H.-C. Chang and W. Fann, *Proc. Natl. Acad. Sci.,* 2007, **104**, 727-732.

[244] S.-J. Yu, M.-W. Kang, H.-C. Chang, K.-M. Chen and Y.-C. Yu, *J. Am. Chem. Soc.,* 2005, **127**, 17604-17605.

[245] J.-I. Chao, E. Perevedentseva, P.-H. Chung, K.-K. Liu, C.-Y. Cheng, C.-C. Chang and C.-L. Cheng, *Biophys. J.,* 2007, **93**, 2199-2208.

[246] O. Faklaris, D. Garrot, V. Joshi, F. Druon, J.-P. Boudou, T. Sauvage, P. Georges, P. A. Curmi and F. Treussart, *Small,* 2008, **4**, 2236-2239.

[247] O. Faklaris, V. Joshi, T. Irinopoulou, P. Tauc, M. Sennour, H. Girard, C. Gesset, J.-C. Arnault, A. Thorel ,J.-P. Boudou, P. A. Curmi and F. Treussart, *ACS Nano,* 2009, **3**, 3955-3962.

[248] E. Perevedentseva, S.-F. Hong, K.-J. Huang, I.-T. Chiang, C.-Y. Lee, Y.-T. Tseng and C.-L. Cheng, *J. Nanopart. Res.,* 2013, **15**, 1834-1846.

[249] M.-F. Weng, S.-Y. Chiang, N.-S. Wang and H. Niu, *Diamond Relat. Mater.,* 2009, **18**, 587-591.

[250] M. Mkandawire, A. Pohl, T. Gubarevich, V. Lapina, D. Appelhans, G. Rödel, W. Pompe, J. Schreiber and J. Opitz, *J. Biophoton.,* 2009, **2**, 596-606.

[251] K. K. Liu, C.-C. Wang, C.-L. Cheng and J.-I Chao, *Biomaterials,* 2009, **30**, 4249-4259.

[252] C.-Y. Fang, V. Vaijayanthimala, C.-A. Cheng, S.-H. Yeh, C.-F. Chang, C.-L. Li and H.-C. Chang, *Small,* 2011, **7**, 3363-3370.

[253] Y.-K. Tzeng, O. Faklaris, B.-M. Chang, Y. Kuo, J.-H. Hsu and H.-C. Chang, *Angew. Chem. Int. Ed.,* 2011, **50**, 2262-2265.

[254] M.-F. Weng, B.-J. Chang, S.-Y. Chiang, N.-S. Wang and H. Niu, *Diamond Relat. Mater.,* 2012, **22**, 96-104.

[255] Y.-C. Lin, L.-W. Tsai, E. Perevedentseva, H.-H. Lin, D.-S. Sun, A. E. Lugovtsov, A. Priesshev, J. Mona and C.-L. Cheng, *J. Biomed. Opt.,* 2012, **17**, 101512.

[256] T.-J. Wu, Y.-K. Tzeng, W.-W. Chang, C.-A. Cheng, Y. Kuo, C.-H. Chien, H.-C. Chang and J. Yu, *Nature Nanotechnol.,* 2013, **8**, 682-689.

[257] Z.-Y. Lien, T.-C. Hsu, K.-K. Liu, W.-S. Liao, K.-C. Hwang, J.-I. Chao, *Biomaterials,* 2012, **33**, 6172-6185.

[258] I. Rehor, J. Slegerova, J. Kucka, V. Proks, V. Petrakova, M.-P. Adam, F. Treussart, S. Turner, S. Bals, P. Sacha, M. Ledvina, A. M. Wen, N. F. Steinmetz and P. Cigler, *Small,* 2014, **10**, 1106-1115.

[259] J. Slegerova, M. Hajek, I. Rehor, F. Sedlak, J. Stursa, M. Hruby and P. Cigler, *Nanoscale,* 2014, DOI: 10.1039/C4NR02776K.

[260] Y. Nawa, W. Inami, S. Lin, Y. Kawata, S. Terakawa, C.-Y. Fang and H.-C. Chang, *ChemPhysChem,* 2014, **15**, 721-726.

[261] K.-K. Liu, W.-W. Zheng, C.-C. Wang, Y.-C. Chiu, C.-L. Cheng, Y.-S. Lo, C. Chen and J.-I. Chao, *Nanotechnol.,* 2010, **21**, 315106.

[262] A. Alhaddad, M.-P. Adam, J. Botsoa, G. Dantelle, S. Perruchas, T. Gacoin, C. Mansuy, S. Lavielle, C. Malvy, F. Treussart and J.-R. Bertrand, *Small,* 2011, **7**, 3087-3095.

[263] Y.-C. Lin, E. Perevedentseva, L.-W. Tsai, K.-T. Wu and C.-L. Cheng, *J. Biophotonics,* 2012, **5**, 838-847.

[264] N. Mohan, C.-S. Chen, H.-H. Hsieh, Y.-C. Wu and H.-C. Chang, *Nano Lett.,* 2010, **10**, 3692-3699.

[265] N. Mohan, B. Zhang, C.-C. Chang, L. Yang, C.-S. Chen, C.-Y. Fang, H.-H. Hsieh, C.-Y. Cho, Y.-C. Wu, J.-H. Weng, B.-c. Chung and H.-C. Chang, *MRS Proceedings,* 2011, **1362**, mrss11-1362-qq06-01.

[266] R. Igarashi, Y. Yoshinari, H. Yokota, T. Sugi, F. Sugihara, K. Ikeda, H. Sumiya, S. Tsuji, I. Mori, H. Tochio, Y. Harada and M. Shirakawa, *Nano Lett.,* 2012, **12**, 5726-5732.

[267] V. Vaijayanthimala, P.-Y. Cheng, S.-H. Yeh, K.-K. Liu, C.-H. Hsiao, J.-I Chao and H.-C. Cheng, *Biomaterials,* 2012, **33**, 7794-7802.

[268] S. K. Sonkar, M. Ghosh, M. Roy, A. Begum and S. Sarkar, *Mater. Express,* 2012, **2**, 105-114.

[269] Z. Liu, M. Winters, M. Holodniy and H. Dai, *Angew. Chem. Int. Ed.,* 2007, **46**, 2023-2027.

[270] C. Lamprecht, N. Gierlinger, E. Heister, B. Unterauer, B. Plochberger, M. Brameshuber, P. Hinterdorfer, S. Hild and A. Ebner, *J. Phys.: Condens. Matter,* 2012, **24**, 164206.

[271] C. Wang, X. Ma, S. Ye, L. Cheng, K. Yang, L. Guo, C. Li, Y. Li and Z. Liu, *Adv. Funct. Mater.,* 2012, **22**, 2363-2375.

[272] X. Wang, C. Wang, L. Cheng, S.-T. Lee and Z. Liu, *J. Am. Chem. Soc.,* 2012, **134**, 7414-7422.

[273] Z. Liu, C. Davis, W. Cai, L. He, X. Chen and H. Dai, *Proc. Natl. Acad. Sci.,* 2008, **105**, 1410-1415.

[274] Z. Liu, K. Chen, C. Davis, S. Sherlock, Q. Cao, X. Chen and H. Dai, *Cancer Res.,* 2008, **68**, 6652-6660.

[275] X. Liu, H. Tao, K. Yang, S. Zhang, S.-T. Lee and Z. Liu, *Biomaterials,* 2011, **32**, 144-151.

[276] S. Keren, C. Zavaleta, A. de la Zerda, O. Gheysens and S. S. Gambhir, *Proc. Natl. Acad. Sci.,* 2008, **105**, 5844-5849.

[277] C. Zavaleta, A. de la Zerda, Z. Liu, S. Keren, Z. Cheng, M. Schipper, X. Chen, H. Dai and S. S. Gambhir, *Nano Lett.,* 2008, **8**, 2800-2805.

[278] C.-Y. Cheng, E. Perevedentseva, J.-S. Tu, P.-H. Chung, C.-L. Cheng, K.-K. Liu, J.-I. Chao, P.-H. Chen and C.-C. Chen, *Appl. Phys. Lett.,* 2007, **90**, 163903.

[279] H. Omachi, Y. Segawa and K. Itami, *Acc. Chem. Res.*, 2012, **45**, 1378-1389.

[280] J. Xia, J. W. Bacon and R. Jasti, *Chem. Sci.*, 2012, **3**, 3018-3021.

[281] A.-F. Tran-Van and H. A. Wegner, *Beilstein J. Nanotechnol.*, 2014, **5**, 1320-1333.

[282] Y. Segawa, A. Fukazawa, S. Matsuura, H. Omachi, S. Yamaguchi, S. Irle and K. Itami, *Org. Biomol. Chem.*, 2012, **10**, 5979-5984.